MECHANISTIC STUDIES OF AUTOPHAGY INITIATION IN MAMMALIAN CELLS

APPROVED BY SUPERVISORY COMMITTEE

Xiaodong Wang, Ph.D.

Benjamin Tu, Ph.D.

John Abrams, Ph.D.

Jose Rizo-Rey, Ph.D.

DEDICATION

To my late father, Zhiqiang SHANG, and my mother Weiqin GE,

for their unfailing love and support.

ACKNOWLEDGEMENT

This work would not have been possible without the support from many people. First, I would like to thank Dr. Xiaodong Wang for his mentorship. Your expertise in biology and dedication to scientific career are truly inspirational. You have given me tremendous help in many aspects. In particular, you taught me how to think and perform both critically and independently, and guided me head toward relevant, meaningful answers.

To all members of the Wang lab, thank you so much for your help throughout these years. I would especially like to acknowledge Dr. Lai Wang, Dr. Zhigao Wang and Dr. Gelin Wang, for their assistance all the way along my research progresses.

I would like to offer my sincerest thanks to the members of my dissertation committee, including Dr. Benjamin Tu, Dr. John Abrams, and Dr. Jose Rizo-Rey. Thank you so much for taking time out of your busy schedules to assist me with my research. You have made numerous invaluable efforts to keep me on the right track.

Hardly do I know how to start my acknowledgement to my parents. Your love and encouragement have been my all-time best inspirations. You have taught me to adopt optimism strategically for my life and approach all life's problems with integrity and discipline. These lessons are inarguably the best education. Though I did doubt what direction I should take, I never doubted that you were proud of me and always ready to help.

MECHANISTIC STUDY OF MAMMALIAN AUTOPHAGY INITIATION

By

LIBIN SHANG

DISSERTATION

Presented to the Faculty of the Graduate School of Biomedical Sciences

The University of Texas Southwestern Medical Center at Dallas

In Partial Fulfillment of the Requirements

For the Degree of

DOCTOR OF PHILOSOPHY

The University of Texas Southwestern Medical Center at Dallas

Dallas, Texas

February, 2011

MECHANISTIC STUDY OF MAMMALIAN AUTOPHAGY INITIATION

LIBIN SHANG

The University of Texas Southwestern Medical Center at Dallas, 2011

Supervising Professor: Xiaodong Wang, Ph.D.

Macroautophagy (herein referred to as autophagy) is an evolutionarily conserved self-digestive process cells use to adapt to starvation and other stresses. During autophagy, portions of cytoplasmic materials are engulfed into specialized double-membrane structures to form autophagosomes, which then fuse with lysosomes to degrade their cargos and regenerate nutrients.

Initiation of autophagy has been extensively studied in budding yeast *Saccharomyces cerevisiae*. However, various significant differences exist

between yeast and mammals. To pinpoint how mammalian autophagy is initiated, I first adopted proteomic approaches to identify associating partners of Unc-51-like kinase 1 (Ulk1), key initiator for mammalian autophagy. Two novel proteins, mAtg13 and Atg101, were found to interact with Ulk1 stoichiometrically. Knockdown of either mAtg13 or Atg101 led to decreased autophagy, and autophagy could be rescued with exogenous expression, suggesting the two proteins were critical for mammalian autophagy initiation.

I then observed Ulk1 undergoes dramatic dephosphorylation upon starvation, particularly at serine 638 and serine 758. I found phosphorylations of Ulk1 are mediated by mammalian target-of-rapamycin (mTOR) kinase and AMP-activated protein kinase (AMPK). AMPK interacts with Ulk1 in a nutrient-dependent manner, and proper phosphorylations on Ulk1 are crucial for Ulk1/AMPK association, as a single serine-to-alanine mutation (S758A) at Ulk1 impairs this interaction. Compared to its wild-type counterpart, this Ulk1-S758A mutant initiates starvation-induced autophagy faster at early time points, but does not alter the maximum capacity of autophagy when starvation prolongs. With this layer of regulation, mammalian autophagy is capable of responding to environmental changes more promptly than previously considered.

TABLE OF CONTENTS

PRIOR PUBLICATIONS

1. Libin Shang, She Chen, Fenghe Du, Xiaodong Wang, “”,*Proceedings of the National Academy of Sciences, U.S.A*, in press.

2. Gelin Wang, Libin Shang, Anthony W.G. Burgett, Patrick G. harran, Xiaodong Wang, “Diazonamide toxins reveal an unexpected function for ornithine δ-amino transferase in mitotic cell division”, *Proceedings of the National Academy of Sciences, U.S.A*, Vol. 104, 2068-2073, 2007.

3. Libin Shang, Xinjian Liu, Chunhai Fan and Genxi Li, “A nitric oxide biosensor based on horseradish peroxidase/kieselguhr co-modified pyrolytic graphite electrode”, *Annali. di Chimica,* Vol. 94, 457-462, 2004.

4. Libin Shang, Xinjian Liu, Jun Zhong, Chunhai Fan, Iwao Suzuki and Genxi Li, “Fabrication of ultrathin, protein-containing films by layer-by-layer assembly and electrochemical characterization of hemoglobin entrapped in the film”, *Chemistry Letters*, Vol. 32, 296-297, 2003.

5. Libin Shang, Ziyi Sun, Xingwu Wang and Genxi Li, “Enhanced peroxidase activity of hemoglobin in a DNA membrane and its application to

unmediated hydrogen peroxide biosensor", *Analytical Sciences*, Vol. 19, 1537-1539, 2003.

6. Xinjian Liu, Libin Shang, Ziyi Sun, Genxi Li, "Direct electrochemistry of hemoglobin in dimethyldioctadecyl ammonium bromide film and its electrocatalysis to nitric oxide", *Journal of Biochemical and Biophysical Methods*, Vol. 62, 143-151, 2005.

7. Xinjian Liu, Libin Shang, Jiantao Pang and Genxi Li, "A reagentless nitric oxide biosensor based on hemoglobin/polyethyleneimine film", *Biotechnology and Applied Biochemistry*, Vol. 38, 119-122, 2003.

8. Xinjian Liu, Yinxi Huang, Libin Shang, Xiaoyue Wang, Han Xiao, Genxi Li, "Electron transfer reactivity and the catalytic activity of horseradish peroxidase incorporated in dipalmitoylphosphatidic acid films", *Bioelectrochemistry*, Vol. 68, 98-104, 2006.

9. Hui Zhou, Zhong Chen, Rongwu Yang, Libin Shang, Genxi Li, "Direct electrochemistry and electrocatalysis of hemoglobin in lactobionic acid film", *Journal of Chemical Technology & Biotechnology*, Vol. 81, 58-61, 2006.

10. Xinjian Liu, Han Xiao, Libin Shang, Xiaoyue Wang, Genxi Li. "Electrochemical studies of hemoglobin and myoglobin embedded in dipalmitoylphosphatidic acid films", *Analytical Letters*, Vol. 38, 453-462, 2005.

LIST OF FIGURES

LIST OF TABLES

LIST OF ABBREVIATIONS

IP	immunoprecipitation
HSP	heat shock protein
Ulk	Unc-51-like kinase
FIP200	focal adhesion kinase family interacting protein of 200 kD
RB1CC1	retinoblastoma 1-inducible coiled-coil 1
Tet	tetracycline
Dox	doxycycline
LC3	microtubule-associated protein (MAP) light chain 3
LLPD	long-lived protein degradation
TOR	target-of-rapamycin
TORC1	TOR (target-of-rapamycin) complex 1
MEF	mouse embryonic fibroblast
AMPK	AMP-activated kinase
PI3K	Phosphoinositide 3-kinase

LKB1	Serine/threonine kinase 11, STK1
TSC	tuberous sclerosis complex
Rheb	Ras homolog enriched in brain
Akt/PKB	protein kinase B
PTEN	phosphatase and tensin homolog

I. BACKGROUND INTRODUCTION

Abstract

Eukaryotic cells have evolved various signaling cascades and cellular processes in response to rapid environmental changes. Among these, macroautophagy (herein referred to as autophagy) is an evolutionarily conserved self-digestive process cells use to adapt to nutrient starvation. It also plays crucial roles in development, innate immune defense, protein quality control, tumor suppression, and cell death. During autophagy, portions of cytoplasmic materials are engulfed into specialized double-membrane structures to form autophagosomes, which then fuse with lysosomes to degrade their cargos and regenerate nutrients. This process is highly inducible and tightly regulated. Under normal growth conditions where nutrients are abundant, autophagy is kept at a basal level mainly for house-keeping purposes such as degradation of long-lived proteins and turn-over of damaged cellular organelles; under stress conditions like nutrient starvation, autophagy is further induced to provide cells with additional internal nutrient supplies. This induction is largely due to inhibition of TOR (target-of-rapamycin) complex 1 (TORC1), a kinase complex whose activity is regulated through integrating upstream PI3K

(phosphatidylinositol 3-kinase)/AMPK (AMP-activated protein kinase) activities and other nutrient-sensing signalings.

Introduction

Homeostasis of eukaryotic cells involves a dynamic balance between synthesis and degradation. There are two major mechanisms for the turnover of protein/organelle in eukaryotic cells. The first one is the ubiquitin-proteosome pathway, well characterized for rapid degradation of unwanted proteins (Finley, 2009; Schwartz and Ciechanover, 1999). The second one is through lysosomal degradation. The lysosome, or its yeast/plant counterpart the vacuole, uses a variety of resident acid hydrolases to degrade damaged organelles, long-lived proteins, and invasive pathogens (He and Klionsky, 2009).

Autophagy is adopted by eukaryotes as a response to unfavorable conditions such as nutrient starvation. It is a highly regulated self-digesting process using lysosomes. During autophagy, a certain kind of vesicles termed autophagosomes, form inside cell. Various cargos are recognized and engulfed by autophagosomes, including long-lived proteins, damaged organelles, and invasive pathogens. These cargos are then transported into lysosomes for degradation. Autophagosomes have a unique double-membrane structure.

When targeted to lysosomes, its outer-membrane fuses with the lysosomal membrane. The inner membrane then gets into lysosome and is degraded together with cargos (Figure I-1) (He and Klionsky, 2009).

Lysosomal degradation generates macromolecules such as amino acids and other cellular "building blocks". These nutrients are released from lysosomes and back to the cytoplasm for re-use, particularly during starvation conditions (Yorimitsu and Klionsky, 2005). Proper autophagy is important for cellular homeostasis, as efficient sequestration and clearance of damaged/unwanted cellular components are critical for cell survival and function. Malfunction of autophagy can lead to many diseases, including neurodegenerative diseases, cardiovascular disorders, microbe infections, and cancers (Kroemer et al., 2010; Sumpter and Levine, 2010; Wong and Cuervo, 2010).

Here I roughly categorize autophagy research into three stages. The first stage is from 1950s to 1992/1993. In this period of time, autophagy was part of studies of lysosome function and was mainly observed in mammalian systems (such as liver). The major approach was to use electron microscopy (EM). The definition of autophagy was given as "the process of bulk degradation of cytoplasmic proteins or organelles in the lytic compartment", and

autophagosomes were observed by EM in mammalian cells since as early as the 1950s (De Duve and Wattiaux, 1966; Klionsky, 2007; Mortimore et al., 1989; Schworer et al., 1981).

The second stage for autophagy research began from 1992/1993 and lasted till 1998/1999, when the molecular machinery for autophagy and its regulation started to be thoroughly investigated. The breakthroughs were primarily from genetic screens in the budding yeast *Saccharomyces cerevisiae* and the methylotrophic yeasts *Pichia pastoris* and *Hansenula polymorpha*, which led to the identification of a set of autophagy-related (Atg) genes (17 genes till 1999, and 32 genes till today) (Harding et al., 1995; Takeshige et al., 1992; Thumm et al., 1994; Tsukada and Ohsumi, 1993). Based on their interacting partners and functions, these Atg proteins act at several physiologically sequential steps during the autophagy process, including initiation, cargo recognition/packaging, vesicle formation, fusion with lysosomes, and breakdown.

The third stage started from 1998/1999, when Beclin-1, the first mammalian homolog of the yeast autophagy gene Atg6, was reported (Liang et al., 1999; Liang et al., 1998). From then on, more and more researchers started

to study autophagy back in the mammalian systems, and the relationship between autophagy and various diseases has caused much attention.

Autophagy is a highly conserved process through evolution because many Atg homologs have been identified and characterized in higher eukaryotes including human. However, various differences also exists between yeasts and higher eukaryotes such as mammals. For an instance, in yeast, the site where autophagosome starts to form is termed the phagophore assembly site (PAS, also called pre-autophagosomal structure) (Suzuki et al., 2007). Yeast appears to have only one distinct PAS adjacent to the vacuole (the yeast lysosome), whereas in mammals, autophagosomes emerge from multiple sites inside one single cell.

Molecular machinery for autophagy initiation

In yeast, autophagy responds mainly to nutrient availability (Takeshige et al., 1992). Target of rapamycin (TOR), a key regulatory kinase which integrates multiple nutrient signals, is upstream of and participates in the regulation of autophagy. Nutrient starvation, or rapamycin treatment, inhibits kinase activity of TOR and initiates autophagy (Noda and Ohsumi, 1998). TOR protein is able to form two distinct complexes, TOR complex 1 (TORC1) and TORC2 (Wullschleger

et al., 2006). Only TORC1 is sensitive to rapamycin and responsible for regulating autophagy.

Directly downstream of TORC1 is the Atg1 kinase and its associating regulators — Atg13, Atg17, Atg29 and Atg31 (Figure I-2). These factors comprise the most upstream Atg subfamily and collaboratively act at the initiation step of autophagy. Atg1 is a serine/threonine protein kinase whose kinase activity is required for proper autophagy (Matsuura et al., 1997). When cells are fed, the kinase activity of Atg1 stays low, and autophagy is kept at a basal level (Kamada et al., 2000). Upon nutrient starvation or rapamycin treatment, the kinase activity of Atg1 is greatly enhanced. This enhancement requires yeast Atg13, a nutrient-dependent associating partner of yeast Atg1 kinase (Kamada et al., 2000). Atg13 is directly phosphorylated in a TORC1-dependent manner under nutrient-rich condition and is rapidly dephosphorylated by multiple phosphatases in response to starvation and/or rapamycin treatment (Funakoshi et al., 1997; Kamada et al., 2000). Dephosphorylated Atg13 associates much stronger with Atg1 and this Atg1/Atg13 interaction, through unknown mechanism(s), leads to a dramatic elevation of kinase activity of Atg1. It is believed that phosphorylation of one or more proteins by Atg1 kinase is crucial for triggering downstream autophagic events and several Atg proteins have been

reported both *in vivo* and *in vitro* to be phosphorylated in an Atg1-dependent manner, yet the physiological significance of the phosphorylation of these proteins remains unclear, and the direct substrate(s) of Atg1 kinase is still unknown.

Atg13 was recently reported to be a direct target of TORC1, and dephosphorylation of Atg13 is sufficient for the induction of autophagy (Kamada, 2010). Atg13 is directly phosphorylated by TORC1 *in vitro* at multiple (at least 8) serine residues. Moreover, expression of an unphosphorylatable Atg13 mutant (with 8 serine-to-alanine mutations) partially initiates autophagy even when cells are well fed (and TOR is active), suggesting that dephosphorylation of Atg13 is sufficient for autophagy induction.

In yeast, Atg1 and Atg13 are core components of autophagosome formation, while Atg17, Atg29 and Atg31 respond specifically to nutrient deprivation signals (Kabeya et al., 2005; Kabeya et al., 2007; Kamada et al., 2000; Kawamata et al., 2008; Kawamata et al., 2005). The latter three proteins form a constitutive complex and this ternary complex associates with Atg1/Atg13 core complex in a starvation-dependent manner. This event is critical for the full activation of the kinase activity of Atg1 and recruitment of other Atg proteins to

the PAS (Cheong et al., 2008; Kabeya et al., 2005). Interestingly, these five proteins can form a complex in yeast using kinase-dead Atg1, indicating that instead of inducing complex formation, the kinase activity of Atg1 acts at other steps of autophagy (Cheong et al., 2008; Kawamata et al., 2008). Indeed, it has been reported that in the absence of Atg1's kinase activity some Atg proteins abnormally localize to PAS, while others fail to target to PAS, suggesting that the kinase activity of Atg1 is important for proper shuttling of Atg proteins at the PAS (Cheong et al., 2008; Kawamata et al., 2008; Sekito et al., 2009).

Mammalian homologues of the Atg1 complex have been reported, and regulation of mammalian autophagy initiation is thought to be conserved, also through TORC1/Atg1 signaling (Kuroyanagi et al., 1998; Okazaki et al., 2000). Though similar to their yeast counterpart, the detailed machinery and regulation involved in autophagy initiation have not been investigated until recently (Table I-1). Unc-51-like kinase 1 (Ulk1), as well as the less-studied Ulk2, are two mammalian functional homologs of yeast Atg1 kinase. Similar to yeast Atg1, Ulk1 kinase interacts with several autophagy-related partners, including mammalian Atg13 (mAtg13), Atg101, and FIP200/RB1CC1 (focal adhesion kinase family interacting protein of 200 kD, or retinoblastoma 1-inducible coiled-coil 1) (Chan et al., 2009; Chang and Neufeld, 2009; Ganley et al., 2009; Hosokawa et al.,

2009a; Hosokawa et al., 2009b; Jung et al., 2009; Mercer et al., 2009). Despite these similarities between yeast and mammalian autophagy initiating complexes, significant differences remain between these two systems. FIP200/RB1CC1 and Atg101 are not present in the budding yeast *S. cerevisiae*. As for FIP200/RB1CC1, it may functionally overlap with both yeast Atg11 and yeast Atg17 (Mizushima, 2010). Most importantly, mAtg13 constantly associates with Ulk1 regardless of nutrient availability, which is different from the starvation-induced association between Atg1 and Atg13 in *S. cerevisiae* (Chan et al., 2009; Chang and Neufeld, 2009; Ganley et al., 2009; Hosokawa et al., 2009a; Hosokawa et al., 2009b; Jung et al., 2009; Mercer et al., 2009). Since this dynamic interaction between Atg1 and Atg13 is a key regulatory step for yeast autophagy initiation and is not present in the Ulk1 complex, the mammalian autophagy needs to be initiated in a way that, at least partially, differs from that in yeast (Figure I-3, Figure I-4).

Autophagy regulation by TORC1

TORC1 is able to sense and integrate at least four different types of upstream signals, including amino acids, growth factors, cellular energy status (ADP/ATP ratio), and various stresses (e.g. hypoxia) (Wullschleger et al., 2006).

Below I briefly describe the impact on TORC1 by amino acids and growth factors (Figure I-5).

Amino acids

In the case of amino acid sensing, a recent study has shown that extracellular amino acids enter cells via transporters such as SLC1A5 (solute carrier family 1 member 5) and SLC7A5 (Nicklin et al., 2009). It is not fully clear what is the molecular linkage between amino acid availability and TORC1, yet several reports have shown that Rag proteins, with assistance of a protein complex called Ragulator, activate TORC1 in response to amino acids by mediating translocation of TORC1 to the lysosome, where the TORC1 activator Rheb resides (Ras homolog enriched in brain) (Kim et al., 2008; Sancak et al., 2010; Sancak et al., 2008). Besides these facts, several recent observations indicate that amino acids can also activate mTOR via class III PI3K (hVps34) (Byfield et al., 2005; Nobukuni et al., 2005). Presence of amino acids stimulates hVps34, which leads to mTOR activation and autophagy inhibition.

Growth factors

In high eukaryotes like *Drosophila* and mammals, many hormone-sensing pathways converge on TOR. Autophagy can be induced in the presence of

sufficient amino acids if growth factors are depleted from the extracellular milieu. Insulin, and insulin-like growth factors (IGFs), regulate TOR via class I PI3K (Lum et al., 2005). For instance, the insulin receptor is autophosphorylated on its tyrosine residues upon insulin binding. This leads to recruitment and subsequent phosphorylation of IRS1 and IRS2 (insulin receptor substrate 1 and 2), which form a docking scaffold that allows binding of class I PI3K (p85 subunit). Generation of PIP_3 (phosphatidylinositol (3,4,5)-trisphosphate) by the class I PI3K then increases membrane localization of PKB/Akt and PDK1 (phosphoinositide-dependent protein kinase 1), leading to phosphorylation and activation of PKB/Akt by PDK1 (Alessi et al., 1997; Stokoe et al., 1997). PTEN (3'-phosphoinositide phosphatase) reverses downstream PKB/Akt signaling by decreasing PIP_3 production, and thus positively regulates autophagy (Arico et al., 2001).

TOR and autophagy initiation

The TORC1 signaling cascade is the most important upstream regulation for autophagy. TORC1 is sensitive to rapamycin inhibition. Rapamycin treatment inhibits TORC1 and stimulates autophagy even in the presence of nutrients, suggesting TORC1 signaling negatively regulates autophagy (Noda and Ohsumi, 1998).

In yeast, when nutrients are abundant, TOR directly phosphorylates Atg13. As described previously, phosphorylation of Atg13 impairs the Atg1/Atg13 interaction and decreases the kinase activity of Atg1. Therefore autophagy is kept at a low basal level. When cells are starved, TOR is inactivated, phosphorylation of Atg13 decreases and Atg1/Atg13 association increases. All these events lead to activation of Atg1 and induction of autophagy.

In higher eukaryotes including mammals, Atg13 constantly associates with Atg1 kinase and phosphorylation of Atg13 does not respond to nutrient availability same as in yeast. Therefore TOR has less effect on Atg13 proteins but the negative regulation of TOR toward autophagy is well conserved, indicating that TOR could phosphorylate other Atg proteins in these organisms and initiate autophagy. Atg1 kinase is a good candidate to be a substrate of TOR, either directly or indirectly.

Besides regulating the Atg1 complex, yeast studies also suggest that TORC1 can suppress autophagy via phosphorylation of Tap42, which in turn activates the catalytic subunits of PP2A (the serine/threonine protein phosphatase 2A), a negative regulator of autophagy (Yorimitsu et al., 2009). Downstream targets of PP2A have not been identified. It is possible that Atg

proteins may be directly involved, such as the components in Atg1 kinase complex and other phosphorylated Atg proteins.

Involvement of AMPK in autophagy (Figure I-5)

It has been well documented that metabolic stresses, particularly low cellular energy, can lead to activation of autophagy, and the underlying pathways are understood in considerable detail. In mammals, AMPK (5'-AMP-activated protein kinase) senses the AMP/ATP ratio which reflects low cellular energy status. AMPK is activated by the upstream LKB1 kinase (encoded by the Peutz-Jeghers syndrome gene). Active AMPK leads to phosphorylation and activation of the tuberous sclerosis (TSC1/2) complex, which inhibits mTOR activity through Rheb (Inoki et al., 2003b).

Activated PKB/Akt promotes phosphorylation of TSC2 and blocks TSC1/TSC2 interaction and TSC1/2 complex formation (Manning et al., 2002), which causes Rheb to exist in the active GTP-bound form (Inoki et al., 2003a; Zhang et al., 2003) and allows it to directly bind and activate mTORC1 (Long et al., 2005). When hormones are absent, mTOR is inactivated, and the inhibitory effect on autophagy is removed.

Down-regulation of TORC1 induces autophagy and autophagy helps to promote ATP production via recycling of nutrients. In addition, the LKB1-AMPK pathway also phosphorylates and activates $p27^{kip1}$, a cyclin-dependent kinase inhibitor responsible for cell cycle arrest, which is crucial to prevent cells from undergoing apoptosis and to promote autophagy initiation (Liang et al., 2007). The yeast homolog of mammalian AMPK, Snf1, also positively contributes to autophagy, possibly via independent mechanisms involving Atg1 regulation (Wang et al., 2001).

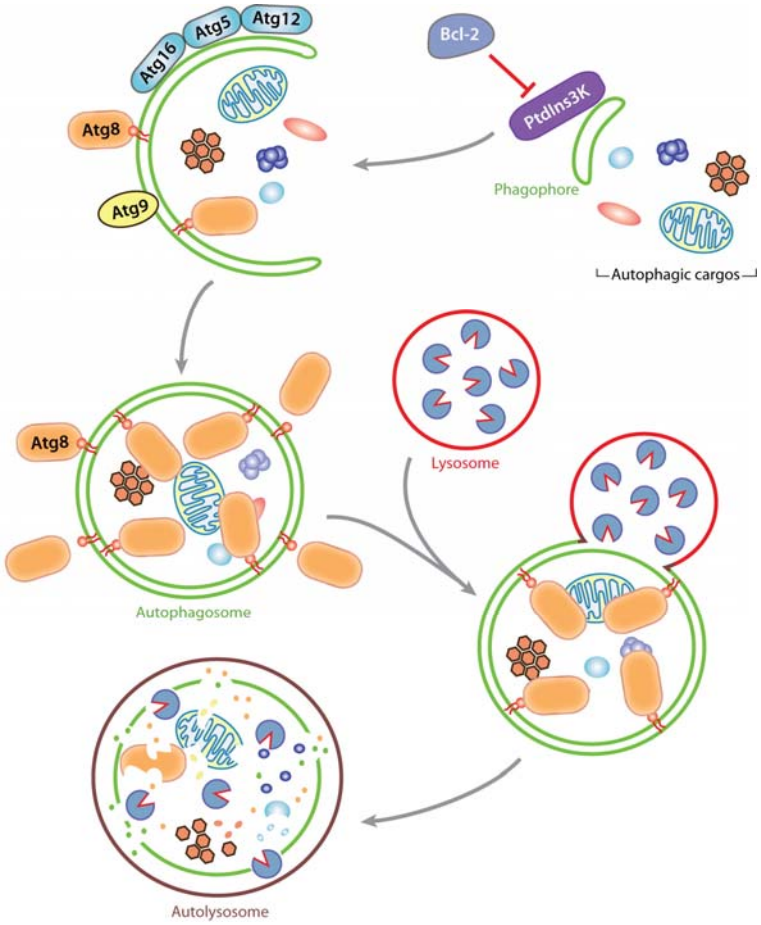

Figure I-1

Schematic model of autophagy. The class III PI3K complex mediates nucleation of the phagophore membrane, enwrapping proteins, damaged organelles and invasive pathogens. Bcl-2 inhibits this step by binding to and confining Beclin-1, a component in the PI3K complex. End products from two conjugation systems, Atg12/Atg5/Atg16 and Atg8–PE conjugates (LC3II in mammalian systems) are also recruited, together with the transmembrane protein Atg9, facilitating the expansion of phagophores. Most of the Atg proteins are dissociated from the autophagosomes upon vesicle completion, allowing fusion between autophagosome and lysosomes, and subsequent cargo degradation by lysosomal proteases. (Figure & legend are adapted/modified from He and Klionsky, 2009)

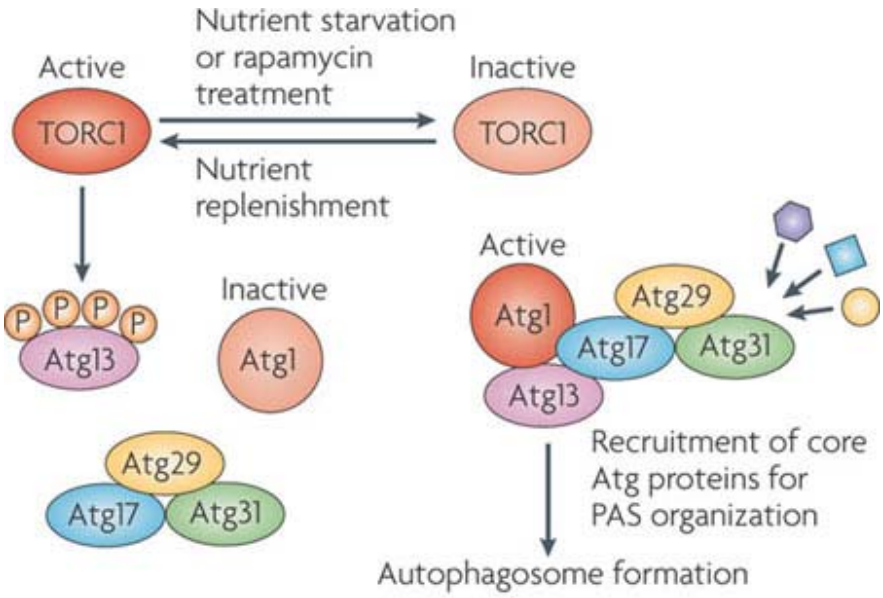

Figure I-2

When target of rapamycin complex 1 (TORC1) is inactivated following nutrient depletion or rapamycin treatment, autophagy-related 13 (Atg13) is dephosphorylated. This allows the association of Atg1 subfamily proteins with Atg13, followed by the upregulation of the Atg1 kinase activity and recruitment of other core Atg proteins to the pre-autophagosomal structure (PAS) to initiate autophagosome formation. These events are immediately reversed on the addition of nutrients. (Figure & legend are adapted/modified from Nakatogawa et al., 2009)

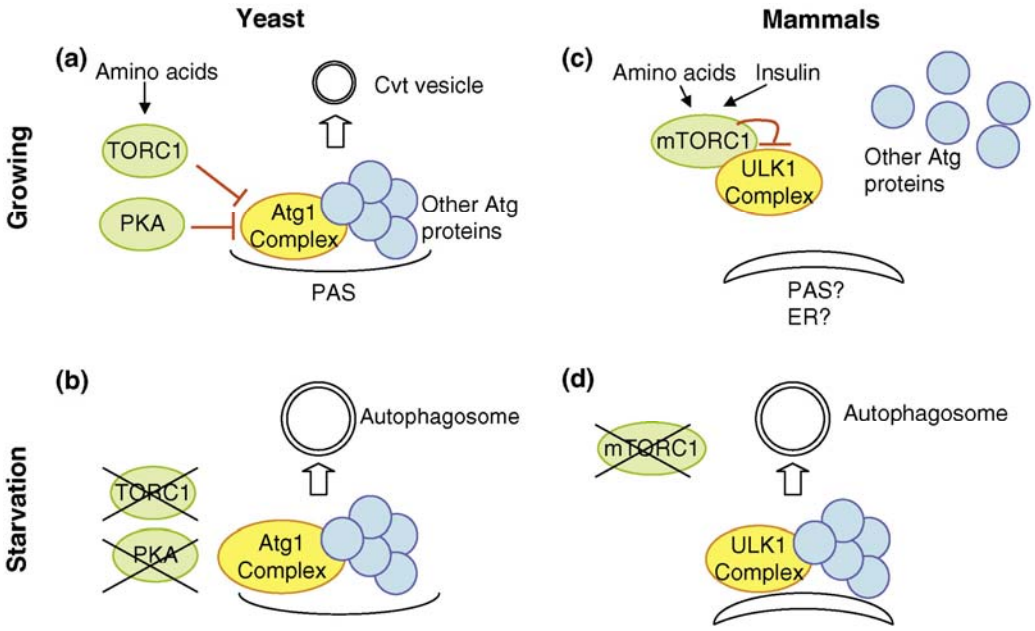

Figure I-3

Comparison of the Atg1/ULK1 complexes between yeast and mammals. (a) In yeast, most Atg proteins accumulate at the PAS and generate Cvt vesicles under growing conditions. The Atg1 protein complex is inactivated by TORC1 and PKA. (b) Upon cell starvation, TORC1-mediated and PKA-mediated Atg1 suppression is lost, leading to Atg1 complex formation, activation, and subsequent autophagy. Recruitment of other Atg proteins is Atg1 kinase-independent, but autophagosome formation requires Atg1 kinase activity. (c) In mammals, mTORC1 directly interacts with the ULK1 complex (ULK1–Atg13–FIP200–Atg101) to inhibit the membrane targeting of the ULK1 complex and other Atg proteins. (d) During starvation, mTORC1 dissociates from the ULK1 complex, allowing it to associate with the mammalian PAS equivalent or endoplasmic reticulum and initiate autophagosome formation. (Figure & legend are adapted/modified from Mizushima, 2010)

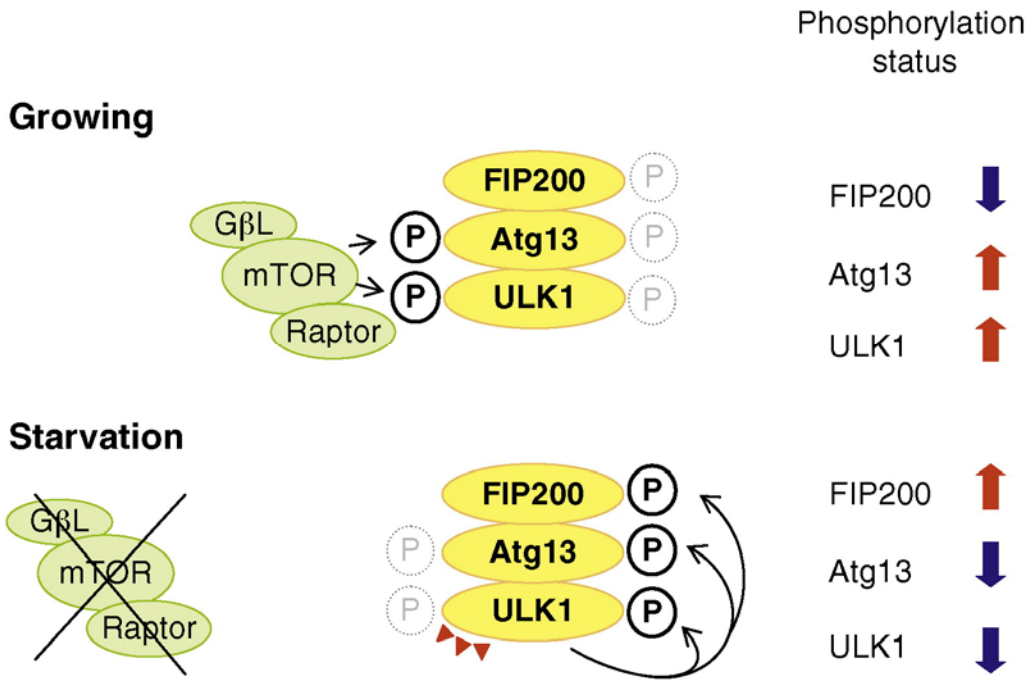

Figure I-4

The phosphorylation status of the ULK1 complex regulates autophagy in mammalian cells. The phosphorylation status of ULK1, mAtg13, and FIP200 changes with cellular nutrient conditions. (Figure & legend are adapted/modified from Mizushima, 2010)

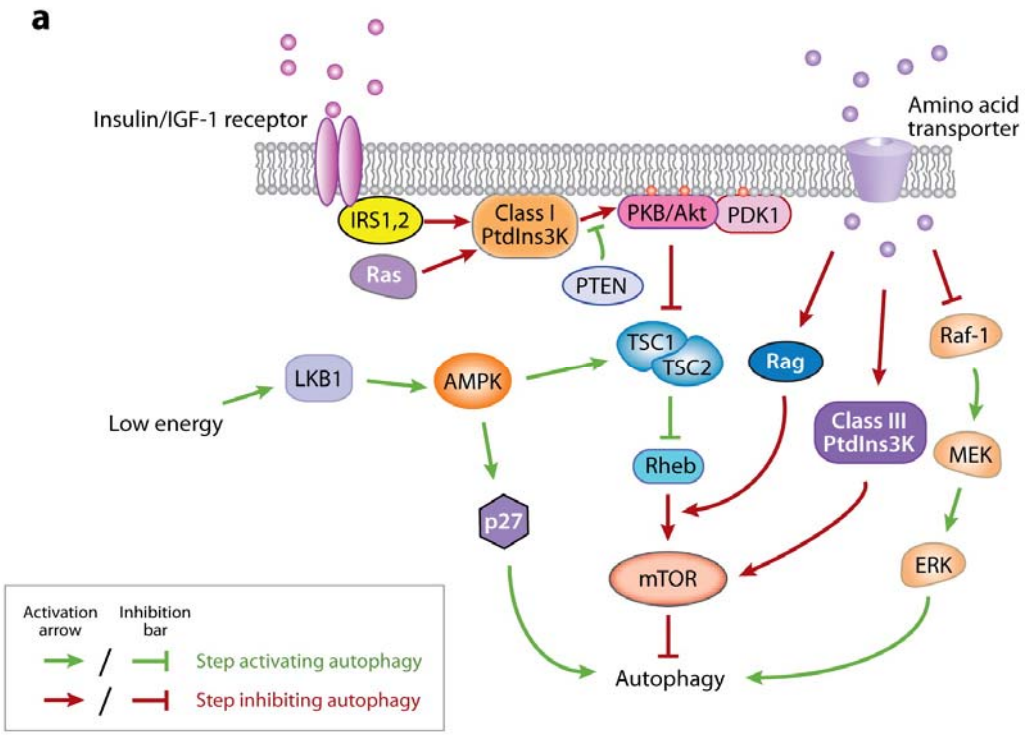

Figure I-5

Regulatory pathways of autophagy by amino acids, hormones, and energy in mammals. (Figure & legend are adapted/modified from He and Klionsky, 2009)

	S. cerevisiae	*S. pombe*	*C. elegans*	*D. melanogaster*	*H. sapiens*
Atg1	Atg1	Atg1	Unc-51	Atg1	ULK1, ULK2
Atg13	Atg13	Atg13	Atg13/Epg1	Atg13	Atg13
Atg17	Atg17	Atg17?	–	–	–
Atg29	Atg29	–	–	–	–
Atg31	Atg31	–	–	–	–
FIP200	–	Taz1IF1?[a]	NP_509241.1	XP_002098061	FIP200/RB1CC1
Atg101	–	Mug66?	NP_741338	NP_573326	Atg101
Atg11	Atg11	Taz1IF1?[a]	–	–	–
Tor	Tor1, Tor2	Tor1, Tor2	Tor	dTor	mTor

Table I-1

Homologs of the Atg1 protein complex subunits (Table is adapted/modified from Mizushima, 2010)

II. IDENTIFICATION OF mAtg13 AND Atg101

Abstract

In this chapter, I independently identified mAtg13 to be the functional homolog of yeast Atg13 by database searching and screening for Ulk1-associating proteins. mAtg13 is shown to constantly interact with Ulk1. Knockdown and rescue experiments prove that mAtg13 is crucial for mammalian autophagy.

I also independently identified another Ulk1-associating protein with molecular weight of 25 kD, which I named p25 and is later reported by two other groups as Atg101 (Hosokawa et al., 2009b; Mercer et al., 2009). Like mAtg13, Atg101 is also found to be essential for proper autophagy induction in mammals.

The study in this chapter defines the role of the Ulk1/mAtg13/FIP200/Atg101 complex as a core autophagy initiating machinery in mammals.

Introduction

The autophagy initiating complex containing Atg1-Atg13-Atg17 has been reported in the budding yeast *Saccharomyces cerevisiae* and is thought to

function downstream of TOR kinase. In this complex, Atg13 is the most regulatable component: it is hyperphosphorylated by TOR under nutrient-rich conditions and rapidly dephosphorylated upon starvation (nitrogen deprivation) or rapamycin treatment. Dephosphorylation of Atg13 facilitates interaction between Atg1 and Atg13. In yeast, both Atg13 and Atg17 are crucial for Atg1 to exhibit its kinase activity and initiate autophagy.

In mammals, Ulk1 and Ulk2 are two functional homologs of yeast Atg1 kinase. FIP200/RB1CC1 interacts with Ulk1/Ulk2 and is considered to have functional overlap with the yeast Atg11/Atg17 protein. Both Ulk1 and FIP200/RB1CC1 have been reported to participate in mammalian autophagy. As to the mammalian homolog of yeast Atg13, a recent bioinformatics study has suggested an unknown protein AAH02378 (NCBI_GENBANK_AC) to be mAtg13. However, the detailed nature (components, necessity, sufficiency, regulation, etc.) of the mammalian autophagy initiating complex remains unclear.

Results and Discussions

Identification of mammalian Atg13 (mAtg13)

To search for mAtg13, I adopted two different approaches. First, I used conventional BLAST to perform a database search. However, it was difficult to

acquire candidates for putative mammalian Atg13 (mAtg13) using the *Saccharomyces cerevisiae* Atg13 sequence as query sequence. I then used the Atg13 sequence from *Schizosaccharomyces pombe* as the query sequence and identified an unknown human protein AAH02378 (NCBI_GENBANK_AC) which has weak homology with the yeast Atg13. After identifying AAH02378 as the putative mAtg13 with database search, another group also assigned the protein as human mAtg13. The second approach I used to identify mAtg13 is to look for Ulk1-associating proteins. Human Flag-HA-Ulk1 was stably expressed in HeLa cells, and immunoprecipitates were subject to silver staining and were analyzed by mass spectrometry. I found AAH02378 to be present in the immunoprecipitates (Figure II-1). On the basis of the above data, together with the results described in the following chapters, I named AAH02378 as human mAtg13.

mAtg13 interacts with Ulk1

Human mAtg13 protein has no known domains/motifs. It has very little sequence identity (16%) compared with *Saccharomyces cerevisiae* Atg13, and contains no Q-rich region which is a characteristic feature of the yeast Atg13 protein.

In order to test whether Ulk1 and mAtg13 can interact with each other, I made a HeLa stable cell line that constantly expresses Flag-HA-mAtg13. To reduce false positive hits during immunoprecipitation (IP), I chose those stable clones with very low level of exogenously expressed mAtg13 compared to endogenous mAtg13. The immunoprecipitated mAtg13-containing complex was subject to silver staining and mass spectrometry for protein identification. As shown in Figure II-2, immunoprecipitation with Flag-HA-mAtg13 revealed that mAtg13 interacts with endogenous Ulk1 and FIP200/RB1CC1, two known factors for mammalian autophagy initiation and functional counterparts of yeast Atg1 and Atg11/Atg17, respectively.

I then generated a HeLa stable line that constantly expresses Flag-HA-Ulk1. Again, in order to reduce false positive associations, I chose those clones in which the exogenous Ulk1 has much lower expression level compared to endogenous Ulk1. The immunoprecipitated Ulk1-containing complex was also subject to silver staining and mass spectrometry for identification. As shown in Figure II-1, IP with Flag-HA-Ulk1 revealed that Ulk1 also interacts with endogenous mAtg13 (and FIP200/RB1CC1).

The above reciprocal IP results prove that mAtg13 is a Ulk1-interacting protein, which is also able to interact with FIP200/RB1CC1, another protein involved in mammalian autophagy initiation.

mAtg13 is essential for autophagy

Given that mAtg13 associates with known proteins essential for autophagy, I next examined the function of mAtg13 toward autophagy. A U2OS stable cell line was generated where addition of tetracycline (Tet; or doxycycline, Dox) will induce expression of siRNA against mRNA of mAtg13 and subsequent knockdown of endogenous mAtg13 protein (Figure II-3).

The U2OS cell line was also engineered to bear stable expression of GFP tagged microtubule-associated protein light chain 3 (GFP-LC3). LC3 is a protein that in humans is encoded by the MAP1LC3B gene. The product of this gene is a subunit of neuronal microtubule-associated MAP1A and MAP1B proteins, which are involved in microtubule assembly and are important for neurogenesis. Studies on the rat homolog implicate a role for this protein in autophagy: LC3 is proved to be the mammalian homologue of yeast Atg8 protein and an important marker/effector of autophagy. GFP-LC3 is localized to the autophagosome and therefore forms a punctate pattern during autophagy.

I then tested autophagosome formation in this U2OS stable cell line using GFP-LC3 puncta as readout. GFP-LC3 was detected diffusely in both cytoplasm and nucleus under nutrient-rich condition (Figure II-3). The physiological importance of LC3 present in nucleus remains unknown. Upon medium withdrawal (starvation), GFP-LC3 proteins rapidly form punctate pattern in cytoplasm, indicating massive autophagy induction and consequent autophagosomes formation. Upon addition of Dox, mAtg13 protein was knocked down. Under this situation, very few GFP-LC3 puncta were induced by starvation, indicating autophagosome formation (autophagy induction) is defective in the absence of mAtg13.

Autophagy is responsible for the degradation of long-lived proteins. Measuring the rate of long-lived protein degradation (LLPD) is one of the frequently used approaches to monitor the flux through the autophagic pathway. As shown in Figure II-4, U2OS cells exhibited basal level autophagy in nutrient-rich (fed) conditions. Under this circumstance, LLPD was about 1% of total cellular proteins in a time window of 2 hours. When mAtg13 was knocked down, LLPD was reduced to about half level, indicating that basal autophagy was impaired in the absence of mAtg13. This impairment was more evident when cells were starved. Total medium withdrawal greatly induced autophagy in U2OS

cells. LLPD reached over 3% in 2 hours, which is a 3 – 4 fold induction compared to basal autophagy level when cells were fed. Under this starvation condition, when mAtg13 was knocked down, LLPD was also induced to only 1.5% in 2 hours.

On the basis of endogenous mAtg13 knockdown, I performed rescue experiments by introducing exogenous Flag-mAtg13 back to the U2OS cell line. As shown in Figure II-5, the impairment of GFP-LC3 puncta formation by mAtg13 knockdown was successfully rescured with exogenous Flag-mAtg13. Similarly, the impaired LLPD was also rescued to normal level (1% when cells were fed, 3% when cells were starved, in a 2-hour time window).

In sum, the above knockdown and rescue experiments in both GFP-LC3 formation and LLPD prove the necessity of mAtg13 for inducing proper mammalian autophagy.

Atg101/p25 interacts with Ulk1 constantly

Similar to mAtg13, the Atg101 protein also has no known domains/motifs. It does not have a yeast counterpart based on either sequence similarity/identity and/or functional output.

In order to test whether Ulk1 and Atg101/p25 can interact with each other, I made a HeLa stable cell line that constantly expresses Flag-HA-p25. To

reduce false positive hits during immunoprecipitation (IP), I chose those stable clones with very low level of exogenously expressed Atg101/p25 compared to endogenous Atg101/p25. The immunoprecipitated Atg101-containing complex was subject to silver staining and mass spectrometry for identification. As shown in Figure II-6, immunoprecipitation with Flag-HA-p25 revealed that it interacted with all currently known factors for mammalian autophagy initiation, including endogenous Ulk1, FIP200/RB1CC1 and mAtg13.

Reciprocal pull-down assays done in both HeLa Flag-HA-Ulk1 and HeLa Flag-HA-mAtg13 stable cell lines confirmed the interaction pattern of Atg101/p25. The immunoprecipitated Ulk1-containing complex and mAtg13-containing complex were subject to silver staining and mass spectrometry for identification. As shown in Figure II-1 & Figure II-2, IP with Flag-HA-Ulk1 and Flag-HA-mAtg13 both confirmed interactions with Atg101/p25.

So far I identified an autophagy-related complex containing at least four factors: Ulk1, FIP200/RB1CC1, mAtg13 and Atg101. In all three pull-down assays (Flag-HA-mAtg13, Flag-HA-Atg101, and Flag-HA-Ulk1), some common proteins were also identified as associating partners, such as tubulin, actin, and heat

shock protein 70 (HSP70). The functional consequences of these proteins interacting with this autophagy initiating complex remain to be elucidated.

Atg101/p25 is essential for autophagy

Given that Atg101/p25 associates with known proteins essential for autophagy, I examined its function in autophagy induction. The U2OS cell line stably expressing GFP-LC3 was used to monitor autophagy changes in the presence and absence of Atg101/p25. An siRNA oligo against endogenous Atg101/p25 (or mock control targeting GFP) was used to knock down the mRNA. As shown in Figure II-7, in the presence of Atg101/p25 (cells were transfected with mock control siRNA oligos), upon medium withdrawal (starvation), GFP-LC3 proteins rapidly form punctate pattern in cytoplasm, indicating massive autophagy induction and consequent autophagosomes formation. When cells were transfected with Atg101/p25 siRNA oligos and the protein was successfully knocked down, very few GFP-LC3 puncta were induced by starvation, indicating that autophagosome formation (autophagy induction) is defective in the absence of Atg101/p25.

Therefore besides mAtg13, the novel Atg101/p25 protein, which has no counterpart in yeast, is also crucial for inducing proper mammalian autophagy.

Identification of the novel autophagy-related Atg101/p25 protein suggests that, in mammals, the machinery and regulations of autophagy could be more complicated compared with yeast.

mAtg13 and Atg101/p25 are not tightly regulated by nutrient availability

Initiation of autophagy in the yeast *Saccharomyces cerevisiae* has been extensively studied. The most regulated step in yeast autophagy is the nutrient-dependent interaction between Atg1 kinase and yeast Atg13. I tested whether this regulation is conserved in the mammalian system and the answer, surprisingly, is negative.

As can be seen in Figure II-1 and Figure II-2, the interaction between Ulk1 (functional counterpart of yeast Atg1 kinase) and mAtg13 does not seem to change much. To better confirm this observation, which is inconsistent with the yeast system, I adopted quantitative approaches. SILAC (stable isotope labeling with amino acids in cell culture) was used to quantitatively monitor the interaction between Ulk1 and mAtg13 in response to nutrient availability. As shown in Table II-1, association between Ulk1 and mAtg13 only slightly increased upon starvation.

Using SILAC, I next found that associations of Ulk1 with FIP200 and Atg101/p25 also stayed largely unchanged. Therefore for the mammalian autophagy initiating complex (Ulk1, FIP200/RB1CC1, mAtg13, Atg101/p25), there are no known regulatable interactions. This observation suggests that, in mammals, initiation of autophagy in response to stresses like starvation has to be regulated in a way that is, at least partially, different from what happens in the yeast system.

Experimental Procedures

Reagents and antibodies

pSuperior vector was from Oligoengine. pPUR vector and Tet-system approved fetal bovine serum (FBS) were from Clontech. DMEM was from ATCC. Opti-MEM I and blasticidin were from Invitrogen. Puromycin and neomycin (G418) was from Calbiochem. Doxycycline was from Sigma. Ulk1 and GFP antibodies were from Santa Cruz. Flag M2, HA and actin antibodies were from Sigma. Rabbit and chicken antibodies were raised against recombinant mAtg13 (Pacific Immunology).

Mass spectrometry analysis

The protein gel bands were digested in gel with sequencing grade trypsin (10 ng/μL trypsin, 50 mM ammonium bicarbonate, pH8.0) overnight at 37 ^{o}C. Peptides were extracted with 5% acetic acid/50% acetonitrile and 0.1% acetic acid/75% acetonitrile sequentially and then concentrated to ~20 μL. The extracted peptides were separated by a homemade analytical capillary column (50 μm 10 cm) packed with C18 reverse phase material (YMC 5 μm spherical particles). An Agilent 1100 series binary pump was used to generate HPLC gradient as follows: 0%-5% B in 5 min, 5%-40% B in 25 min, 40%-100% B in 15 min (A = 0.1 M acetic acid in water, B = 0.1 M acetic acid/80% methanol). The eluted peptides were sprayed into a QSTAR XL mass spectrometer (MDS SCIEX) equipped with a nano-ESI ion source. The mass spectrometer was operated in Information Dependent Acquisition (IDA) mode. Ion spray voltage was 2.1 KV. The MS scan was from m/z 400 to 2000. From each MS scan, top three most abundant peaks were selected for MS/MS fragmentation. Each scan was accumulated for 1 sec. The dynamic exclusion time was set as 20 sec.

Protein database search and peptide quantification

The mass spectra were searched against IPI-human database on an in-house Mascot server (Version 2.2, Matrix Science Ltd.). Carbamidomethyl on cysteine was set as fixed modification. Variable modifications included oxidation on methionine, phosphorylation on serine, threonine, and tyrosine. Quantification mode was SILAC double labeled [13C6, 15N2]-lysine and [13C6, 15N4]-arginine. A maximum of three miscleavages was allowed for search. Mass tolerance was 0.2 Da for precursor ion, 0.25 Da for fragment ions. Mascot search results were imported to the open source software MSQuant (http://msquant.sourceforge.net) to calculate ratios of the heavy/light peptide pairs. Quantification results from each peptide were manually checked to ensure their correctness.

Cell culture

All cells used in this study were cultured in Dulbecco's modified eagle medium (DMEM) supplemented with 10% regular FBS or dialyzed FBS, 200ug/ml penicillin and 100ug/ml streptomycin, referred to as "rich medium". Unless indicated otherwise, cells were starved in Hank's buffered salt solution (HBSS, without calcium/magnesium) containing 1% regular medium (for better cell adherence), referred to as "total starvation medium".

Stable cell lines for inducible knockdown and rescue in U2OS cells

Detailed procedure has been described previously (Zhong et al., 2005). In brief, individual stable colonies of U2OS cells that stably express Tet repressor (TetR) were selected in DMEM medium containing 5 g/mL blasticidin to generate U2OS-TetR stable cell lines. Functional siRNA sequences were first cloned into pSuperior vector. Then, multiple copies of shRNA cassette (including H1 promoter and shRNA sequence) were generated and cloned into pPUR vector according to the protocol from Oligoengine and previous report (Zhong et al., 2005). The pPUR construct was transfected into U2OS-TetR cells and individual stable colonies were selected in DMEM medium containing 2 g/mL puromycin. siRNA sequences used in this research were described as follows:

Ulk1: CACTGACCTGCTCCTTAA

mAtg13: GAAGAATGTCCGCGAGTTT

Preparation of cell lysates and immunoprecipitation (IP)

Cells were washed with ice-cold DPBS and then lysed in ice-cold lysis buffer for 20 min. The lysis buffer contains 50mM Tris pH8.0, 137mM NaCl, 1mM EDTA, 10mM sodium fluoride (NaF), 1% Triton X100, 10% glycerol, protease

inhibitors (Roche) and phosphatase inhibitors (Sigma). The cells were then centrifuged at 12000 g for 20 min and pellets were discarded.

For IP assays, dilute lysates to 1 mg/mL final concentration using lysis buffer. Lysates were pre-cleaned with control IgG beads at 4 ^{o}C. At the same time, primary antibodies were incubated with protein A/G beads for 2 hours at room temperature in DPBS containing 5 mg/mL BSA. The protein A/G beads were then washed twice with cold lysis buffer, added into pre-cleaned lysates, and incubated with rotation for 4 hours at 4 ^{o}C. Immunoprecipitates were washed three times using lysis buffer with doubled NaCl concentration (274 mM), and either eluted with Flag or HA peptides, or denatured directly by boiling for 5 min in SDS sample buffer. The precipitated proteins were resolved by SDS-PAGE and visualized either by silver staining or Western blotting.

Long-lived protein degradation(LLPD) assay

Detailed procedure has been described previously (Gronostajski and Pardee, 1984). In brief, U-2 OS cells were plated in 6-well dish with a density of 40000 cells per well and let grow for 3 days. The growth medium was leucine-dropout DMEM (USBiological) supplied by addition of 65μM cold leucine and 1μCi/ml ^{3}H-labeled leucine (Perkin Elmer). In this assay, dialyzed FBS was used to eliminate

leucine from other source. The cells then were washed with regular DMEM medium and let grow for another 48 hours in regular DMEM medium containing 2 mM cold leucine. On next day, the cells were washed and treated with either regular DMEM or total starvation medium for time durations as indicated (10 min, 30 min, or 120 min). After treatment, for the growth medium, collect 1 mL from each well and add with 112 μL of 100% trichloroacetic acid (TCA) to reach 10% TCA concentration; centrifuge the samples at 12000 g for 2 min; take 400 μL of supernatant to measure ^{3}H readout with scintillation counter. For the cells, first wash with DPBS, then 1 mL of 10% TCA was added to each well and incubate the cells at room temperature for 5 min; after fixation, the cells were washed with 10% TCA and dissolved in 0.2 M NaOH; take 400 μL of the lysates to measure ^{3}H readout. Calculate total ^{3}H readout in the medium and total ^{3}H readout within the cells. Then calculate the ratio of released ^{3}H in the medium to the total ^{3}H readout; this represents the degradation percentage in a given time duration.

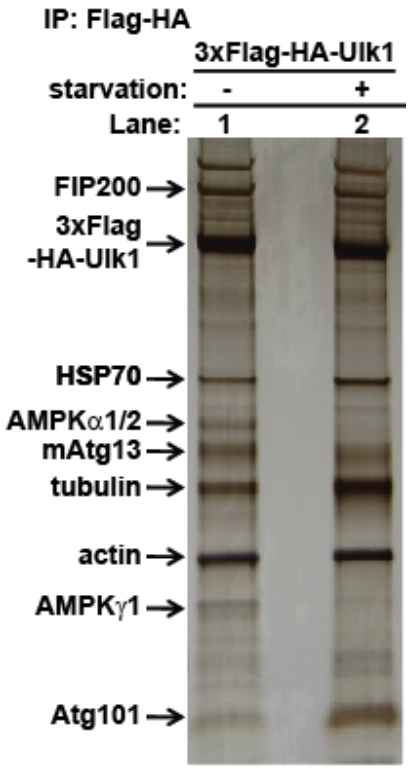

Figure II-1

Ulk1 interacts with other autophagy-related proteins including FIP200, mAtg13, and Atg101. Flag-HA tandem immunoprecipitation (IP) was performed in HeLa cells stably expressing Flag-HA-Ulk1. These interactions are stable and do not respond to nutrient availability. Notably, Ulk1 also interacts with AMPK, but only under nutrient-rich condition. Starvation: cells were starved in HBSS for 2 hrs.

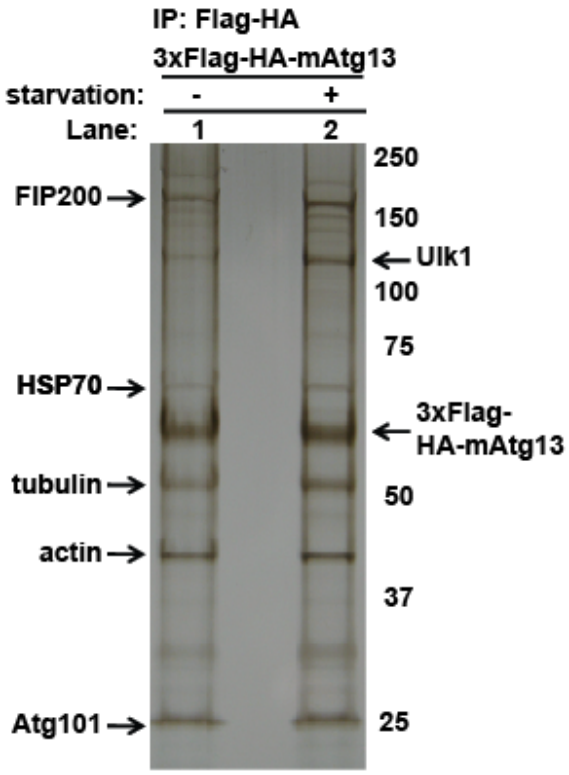

Figure II-2

mAtg13 interacts with other autophagy-related proteins including Ulk1, FIP200, and Atg101. Flag-HA tandem immunoprecipitation (IP) was performed in HeLa cells stably expressing Flag-HA-mAtg13. These interactions are stable and do not respond to nutrient availability. Notably, mAtg13 does not interact with AMPK under any circumstance. Starvation: cells were starved in HBSS for 2 hrs.

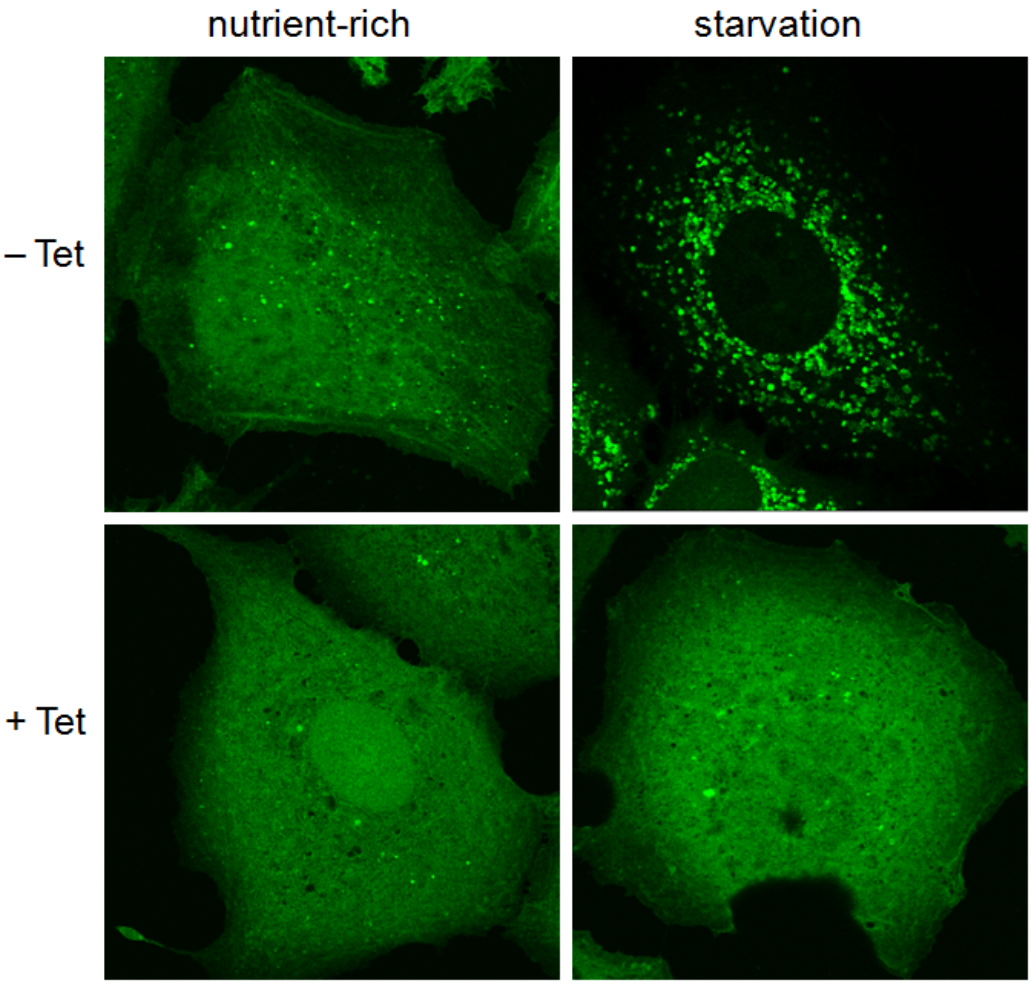

Figure II-3

Knockdown of mAtg13 impairs autophagy. U2OS stable cell line was constructed with constant expression of GFP-LC3 and tetracycline (Tet) inducible expression of shRNA against mAtg13. Starvation: cells were starved in HBSS for 2 hrs.

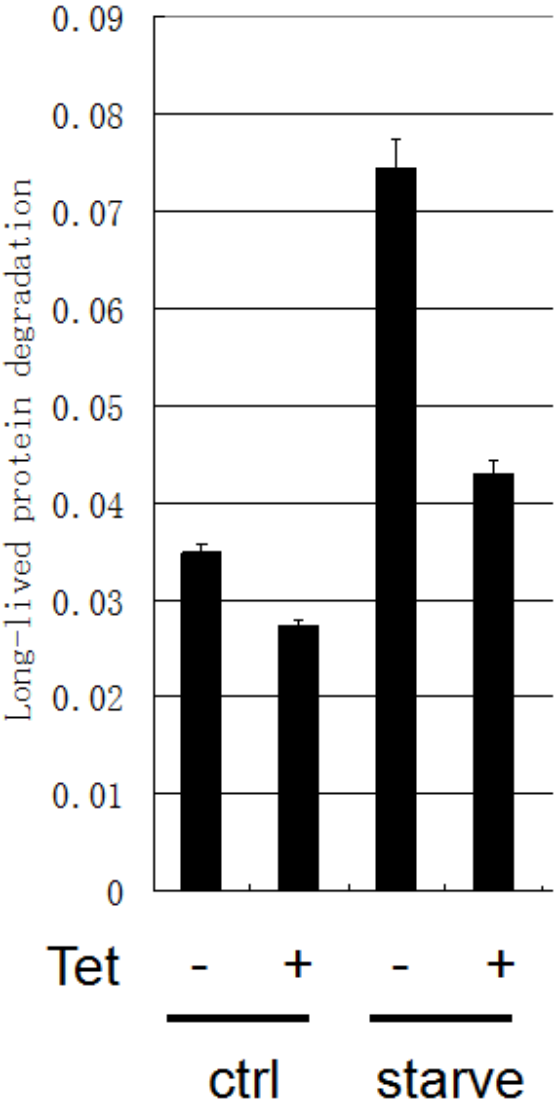

Figure II-4

Knockdown of mAtg13 impairs autophagy. U2OS stable cell line was constructed with tetracycline (Tet) inducible expression of shRNA against mAtg13. Starvation: cells were starved in HBSS for 2 hrs.

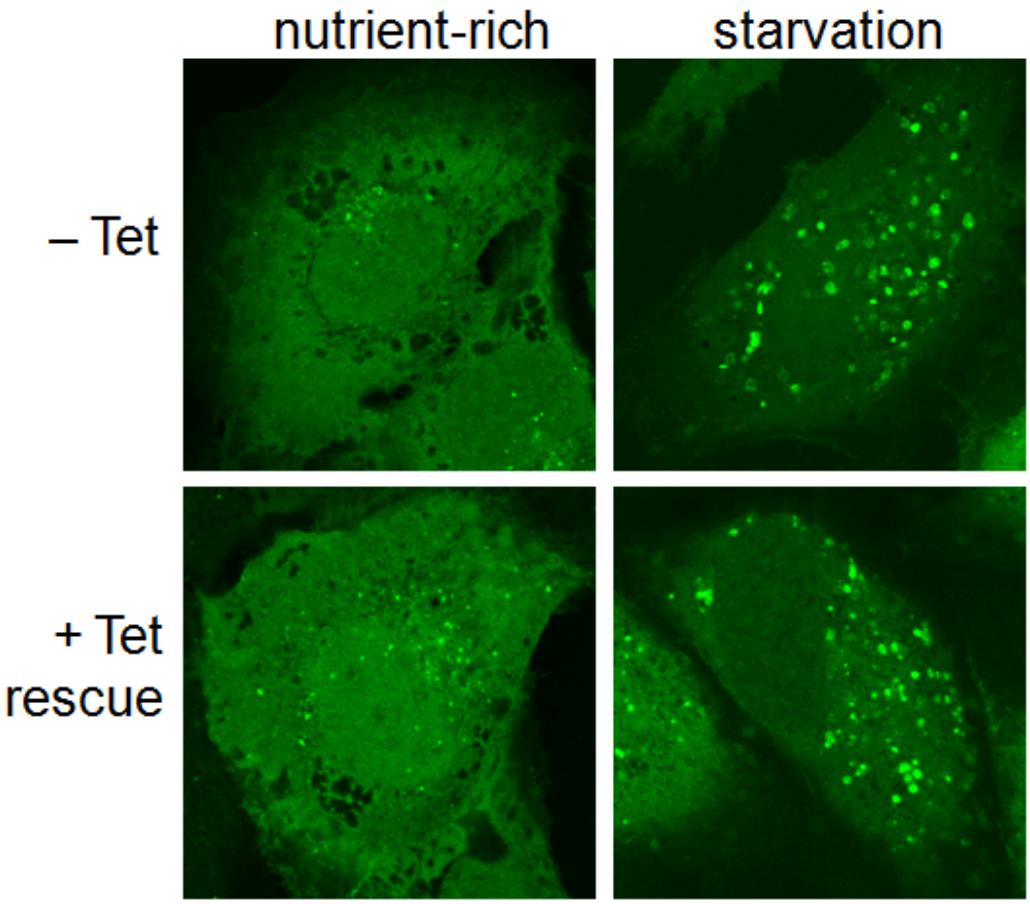

Figure II-5

Rescue experiment confirms necessity of mAtg13 for proper autophagy. U2OS stable cell line was constructed with constant expression of GFP-LC3, tetracycline (Tet) inducible expression of shRNA against mAtg13, and Tet-inducible expression of exogenous Flag-mAtg13 which cannot be targets by the shRNA. Starvation: cells were starved in HBSS for 2 hrs.

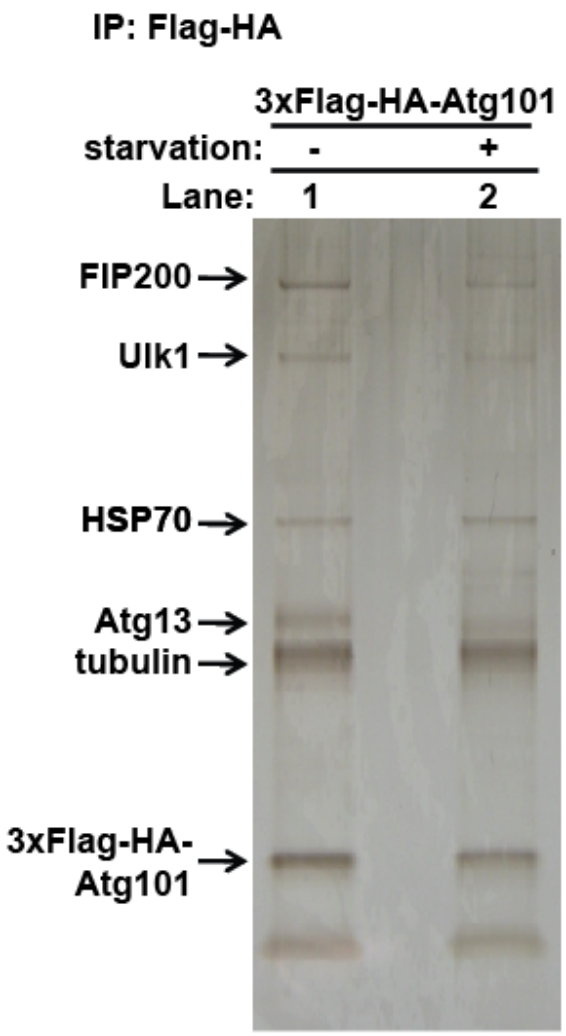

Figure II-6

Atg101/p25 interacts with other autophagy-related proteins including Ulk1, FIP200, and mAtg13. Flag-HA tandem immunoprecipitation (IP) was performed in HeLa cells stably expressing Flag-HA-Atg101/p25. These interactions are stable and do not respond to nutrient availability. Notably, like mAtg13, Atg101/p25 does not interact with AMPK under any circumstance either. Starvation: cells were starved in HBSS for 2 hrs.

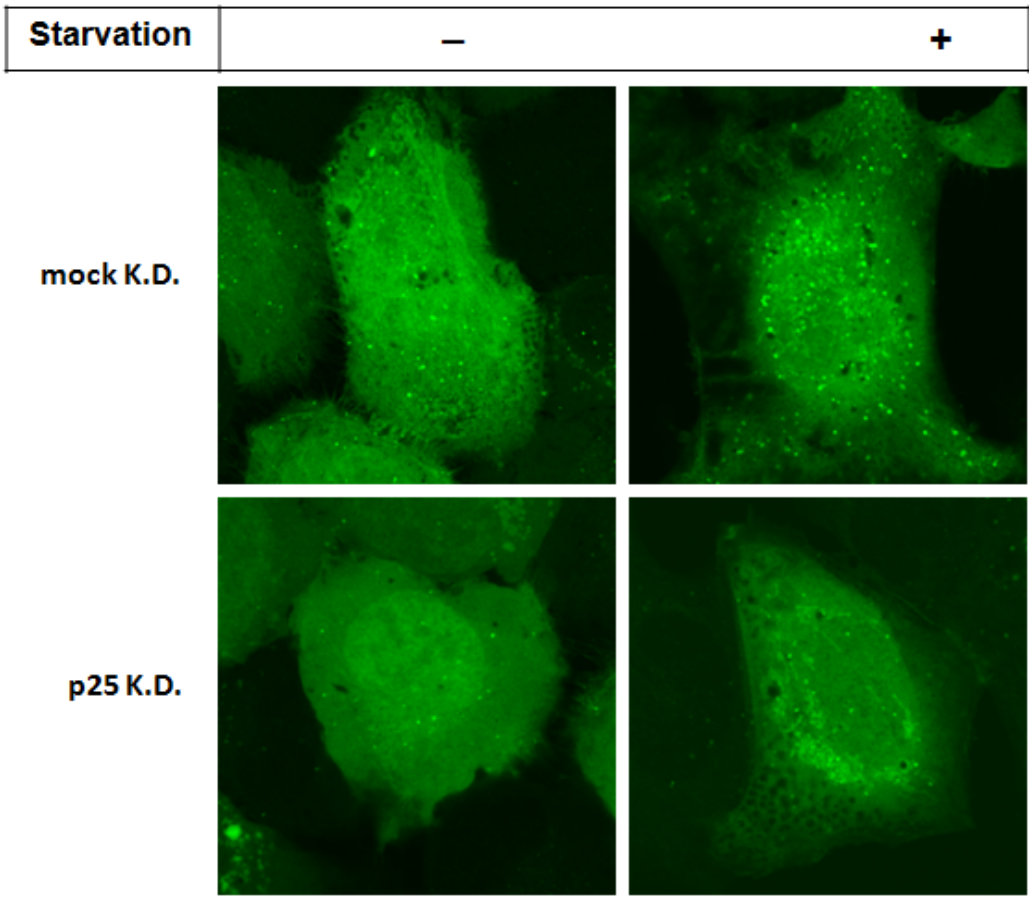

Figure II-7

Knockdown of Atg101/p25 impairs autophagy. U2OS stable cell line was constructed with constant expression of GFP-LC3. The cells were transfected with either shRNA targeting GFP (mock) or Atg101/p25. K.D.: knockdown; starvation: cells were starved in HBSS for 2 hrs.

Accession Number	Protein name	Protein ratio (fed/starved)		
		Corrected to actin (0.92)	Corrected to Ulk1 (0.18)	S.D.
IPI00006080	mAtg13	1.42	1.00	0.13
IPI00289357	ULK1	1.42	1.00	0.28
IPI00783392	FIP200	1.21	0.85	0.10
IPI00305296	Atg101/p25	1.43	1.01	0.18

Table II-1

Quantification of mAtg13 protein complex shows little difference can be observed in terms of association pattern before and after starvation (2 hrs in HBSS). Flag-HA tandem IP was performed in HeLa cells stably expressing Flag-HA-mAtg13, and the final eluate was subject to silver staining followed by SILAC.

III. NUTRIENT-DEPENDENT ULK1 PHOSPHORYLATION REGULATES ULK1/AMPK INTERACTION

Abstract

In the previous chapter I have shown that, regardless of nutrient availability, Ulk1 constantly associates with mAtg13, FIP200/RB1CC1 and Atg101/p25. In this chapter, I investigated whether there exist dynamic Ulk1-associating factors that respond to nutrient availability, which could be the true regulatory molecules for mammalian autophagy initiation. Surprisingly, the AMPK complex falls into this category. I also found that the phosphorylation status of Ulk1 responds to nutrient availability promptly. More importantly, Ulk1 phosphorylation correlates with the Ulk1/AMPK interaction. Ulk1 is highly phosphorylated at serine 638 and serine 758 when cells are fed, and a single serine-to-alanine mutation at serine 758 greatly impairs the Ulk1/AMPK interaction. All these findings indicate that nutrient-dependent Ulk1 phosphorylation regulates the Ulk1/AMPK interaction.

Introduction

Initiation of autophagy has been extensively studied in the budding yeast *Saccharomyces cerevisiae*. Atg1 kinase actively participates in the cytoplasm-to-

vacuole targeting (Cvt) pathway under nutrient-rich condition and switches to induce autophagy upon starvation by forming an autophagy-initiating complex with Atg13, Atg17, Atg29 and Atg31 (Nakatogawa et al., 2009). This event is composed of a signaling cascade including inhibition of yeast TORC1, dephosphorylation of Atg13, increased association between Atg13 and Atg1, and finally, increased Atg1 kinase activity to trigger downstream events. In higher eukaryotes including mammals, though similar to their yeast counterpart, the detailed machinery and regulation involved in autophagy initiation have not been investigated until recently. Unc-51-like kinase 1 (Ulk1), as well as the less-studied Ulk2, are two mammalian functional homologs of yeast Atg1 kinase. Similar to yeast Atg1, Ulk1 kinase interacts with several autophagy-related partners, including mammalian Atg13 (mAtg13), Atg101, and FIP200/RB1CC1 (focal adhesion kinase family interacting protein of 200 kD, or retinoblastoma 1-inducible coiled-coil 1) (Chan et al., 2009; Chang and Neufeld, 2009; Finley, 2009; Ganley et al., 2009; Hosokawa et al., 2009a; Hosokawa et al., 2009b; Jung et al., 2009; Mercer et al., 2009; Mizushima, 2010).

Despite these similarities between yeast and mammalian autophagy initiating complexes, significant differences, however, remain between these two systems. FIP200/RB1CC1 and Atg101 are not present in budding yeast S.

cerevisiae. As for FIP200/RB1CC1, it may functionally overlap with both yeast Atg11 and yeast Atg17 (Mizushima, 2010). Most importantly, mAtg13 constantly associates with Ulk1 regardless of nutrient availability, which is different from the starvation-induced association between Atg1 and Atg13 in S. cerevisiae (Chan et al., 2009; Chang and Neufeld, 2009; Finley, 2009; Ganley et al., 2009; Hosokawa et al., 2009a; Hosokawa et al., 2009b; Jung et al., 2009; Mercer et al., 2009; Mizushima, 2010). Since this dynamic interaction between Atg1 and Atg13 is a key regulatory step for yeast autophagy initiation and is not present in the Ulk1 complex, the mammalian autophagy needs to be initiated in a way that, at least partially, differs from that in yeast.

Results and Discussions

Ulk1 is rapidly phosphorylated upon starvation

Recent studies show that mammalian TORC1 (mTORC1), the upstream regulator of autophagy, may directly interact with the Ulk1 complex under nutrient-rich (fed) conditions and may possibly prevent autophagy initiation through inhibitory phosphorylations (Chan et al., 2009; Chang and Neufeld, 2009; Finley, 2009; Ganley et al., 2009; Hosokawa et al., 2009a; Hosokawa et al., 2009b; Jung et al., 2009; Mercer et al., 2009; Mizushima, 2010). More specific

information including critical phosphorylation residues has not been provided and the functional consequences have not been characterized. SILAC (stable isotope labeling with amino acids in cell culture) was used to quantitatively monitor phosphorylation changes of Ulk1 complex in response to nutrient availability. Unexpectedly, mAtg13 showed little change before and after starvation. Total phosphorylation levels of mAtg13 were low when cells were fed and stayed largely unaltered after starvation (Table III-1). In contrast, Ulk1 was extensively phosphorylated at many residues under nutrient-rich condition and dramatically dephosphorylated upon medium withdrawal (Table III-2). These results suggest that instead of mAtg13, Ulk1 could be the major regulatory component during mammalian autophagy initiation.

In particular, SILAC experiment observed more than 10-fold decreases of phosphorylation at serine 638 and serine 758 of Ulk1, the most significant changes among all phosphorylation sites identified. Phospho-specific antibodies against these two sites were generated and the phosphorylation statuses of these two sites in response to nutrient availability were confirmed. Both serine 638 and serine 758 of Ulk1 were dephosphorylated after starvation as verified by western blotting (Figure III-1A). Mutating these two residues to alanine (S638/758A) mimics the dephosphorylation status, as phospho-specific

antibodies could no longer detect signal on mutant proteins. Mutating these two residues to aspartic acid (S638/758D) could not properly mimic the phosphorylation status of these two sites; the S638/758D mutant behaved similar as S638/758A mutant as test by the phospho-specific antibodies (Figure III-1B).

AMPK associates with Ulk1 in a nutrient-dependent manner

I performed Flag-HA tandem immunoprecipitation (IP) assay in HeLa cells that stably express Flag-HA-Ulk1. The immunoprecipitant was subjected to silver staining followed by mass spectrometry, which identified Atg13, FIP200, and Atg101 to be constantly associated with Ulk1 (Figure II-1, compare lane 1 with lane 2). Surprisingly, AMPK subunits (AMPKα & AMPKγ) were identified to be associated with Ulk1 only under nutrient-rich conditions and were dissociated from Ulk1 upon starvation (Figure II-1). Another AMPK subunit, AMPKβ, did not stain with silver but was indentified there as well by western blotting (see below). I also performed Flag-HA tandem IP in HeLa cells stably expressing either Flag-HA-mAtg13 or Flag-HA-Atg101 and in both assays, Ulk1 and FIP200 were successfully pulled down (Figure II-2, Figure II-6 & Table III-3). However, neither Atg13 nor Atg101 interact with AMPK subunits under any nutrient condition. Similar association patterns were confirmed in HEK 293T cells. Ulk1 interacted

strongly with all three AMPK subunits (AMPKα, AMPKβ & AMPKγ), while Atg13 did not associate with any subunit of AMPK complex (Figure III-2).

Ulk1 does not interact with a constitutively-active form of AMPKα1, which is a truncation from aa1 to aa312 (Figure III-3, upper panel). Neither does Ulk1 interact with the C-terminal part of AMPKα1 (aa312 – C-terminal end) (Figure III-3, middle & lower panels). Therefore, full-length AMPKα is required for its association with Ulk1. The kinase activity of AMPK seems not to be required for its interaction with Ulk1, as Ulk1 was able to interact with a kinase-dead form of AMPKα in the same nutrient-dependent manner (Figure III-4). On the other hand, the kinase domain of Ulk1 (aa1 – aa278) is not required for its interaction with AMPK (Figure III-5). Association between AMPK and the kinase-domain-deleted Ulk1 was still regulated by nutrient availability.

In order to explore this process more quantitatively, SILAC was used to detect the changes in compositions and modifications of mammalian autophagy initiating complex in response to nutrient availability. As shown in Table III-3, association between Ulk1 and Atg13 only slightly increases after starvation. Association of Ulk1 with FIP200/Atg101 also slightly increases. However, the relative amount of these proteins did not change, as would have been predicted

by the yeast model. Similar to the experiments of Figure 1, the amount of Ulk1-associated AMPKα and AMPKγ decreased the most when the medium was withdrawn.

Phosphorylation on Ulk1 dictates the Ulk1/AMPK interaction

Interestingly, AMPK started to dissociate from Ulk1 5 minutes after starvation, and completely re-associated with Ulk1 within 30 min after medium replenishment (Figure III-6). This is in accordance with the time course experiment for Ulk1 phosphorylation (as discussed in next chapter). A series of Ulk1 mutants were then generated to test whether Ulk1/AMPK dissociation upon medium withdrawal is due to dephosphorylation of Ulk1 at these sites. As shown in Figure III-7, mutations at most of residues did not alter the Ulk1/AMPK interaction. However, phosphorylation of Ulk1 at serine 758, one of the most regulated sites as identified by SILAC, is critical for AMPK association. A single mutation at this site (Ulk1-S758A) impaired Ulk1/AMPK interaction, but the residue interaction was still regulated by starvation (Figure III-8). In contrast, single mutation at serine 638 (Ulk1-S638A), the other most regulated site, did not alter Ulk1/AMPK interaction, but it helped further dissociate Ulk1/AMPK when combined with the S758A mutation (Figure III-9).

Experimental Procedures

Reagents and antibodies

Ulk1-S638 and Ulk1-S758 phospho-specific antibodies were generated in rabbit to recognize phosphorylation of Ulk1 at serine 638 and serine 758, respectively (Pacific Immunology).

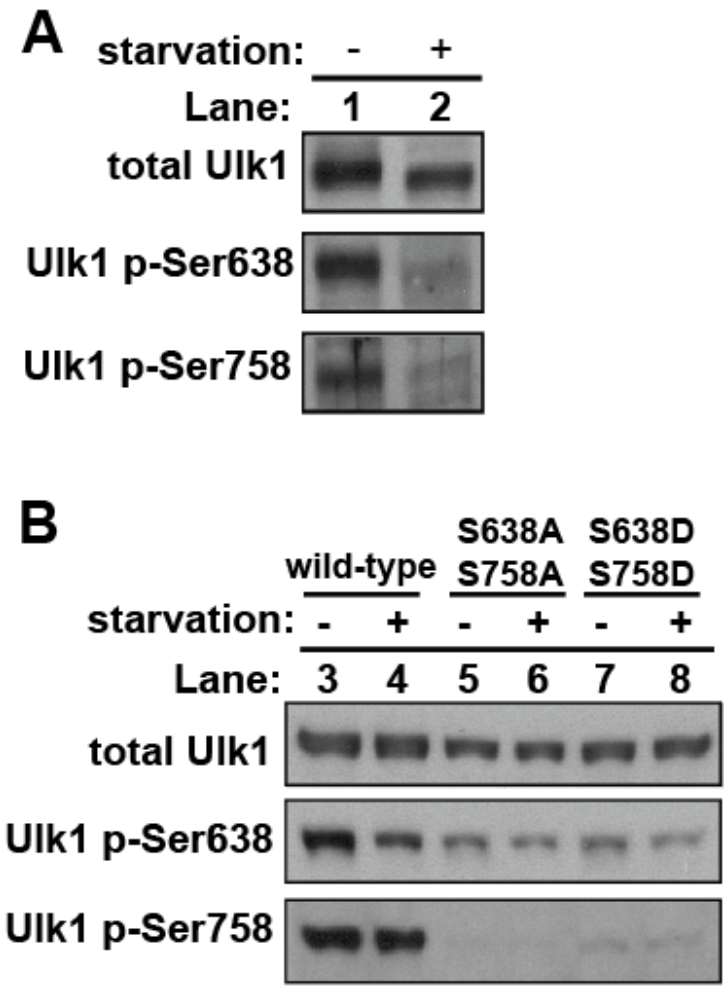

Figure III-1

Verification of phospho-specific antibodies against serine 638 and serine 758 of Ulk1. (A) Phosphorylation of Ulk1 at serine 638 and serine 758 decreases after starvation. Phospho-specific antibodies were generated to recognize S638 and S758 of Ulk1, respectively. U2OS cells were treated for 2 hrs with either rich or total starvation medium. Cell lysates were analyzed by Western blotting. (B) HEK 293T cells were transfected with either Flag-Ulk1 wild-type, Flag-Ulk1 S638A/S758A, or Flag-Ulk1 S638D/S758D, respectively, and were treated and analyzed same as in (A).

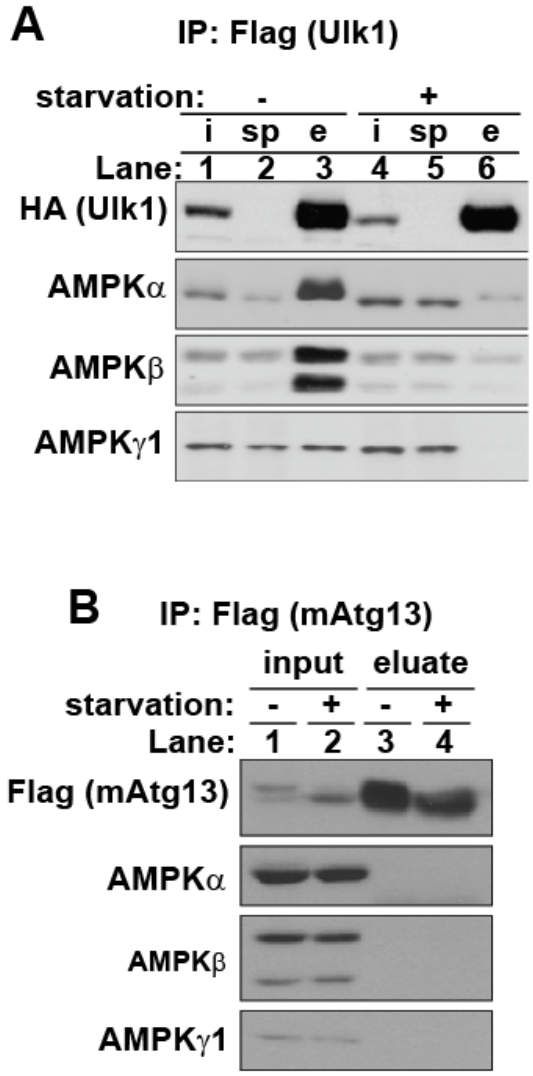

Figure III-2

Investigation of Ulk1/AMPK interaction by immunoprecipitation (IP) assay. (A –B) Ulk1, but not mAtg13, interacts with AMPK in nutrient-dependent manner. HEK 293T cells were transfected with either Flag-HA-Ulk1 (A) or Flag-Atg13 (B). Cells were treated with either rich or total starvation medium for 1 hr, and extracts were immunoprecipitated with anti-Flag beads and eluted with Flag peptide. All 3 subunits of AMPK were pulled down using Flag-Ulk1, while none of them was pulled down using Flag-mAtg13. i: input; sp: soup; e: eluate.

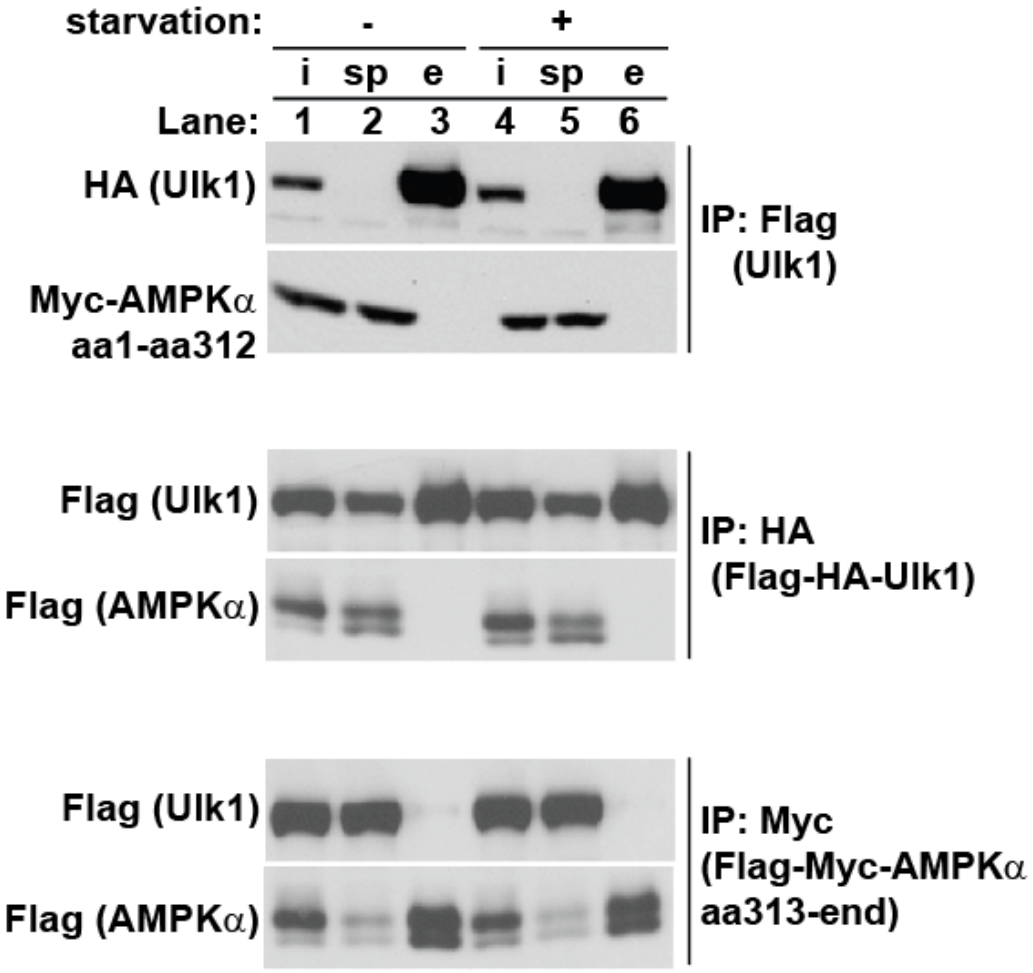

Figure III-3

Full-length AMPKα is required for its interaction with Ulk1. (upper panel) HEK 293T cells were transfected with Flag-HA-Ulk1 and Myc-AMPKα (aa1 – aa312). Cell extracts were immunoprecipitated with anti-Flag beads and eluted with Flag peptide. (middle and lower panel): HEK 293T cells were transfected with Flag-HA-Ulk1 and Flag-Myc-AMPKα (aa312 – C-terminal end). Cell extracts were immunoprecipitated with either anti-HA (middle panel) or anti-Myc (lower panel) beads. The immunocomplexes were eluted with HA peptide and Myc peptide, respectively. i: input; sp: soup; e: eluate.

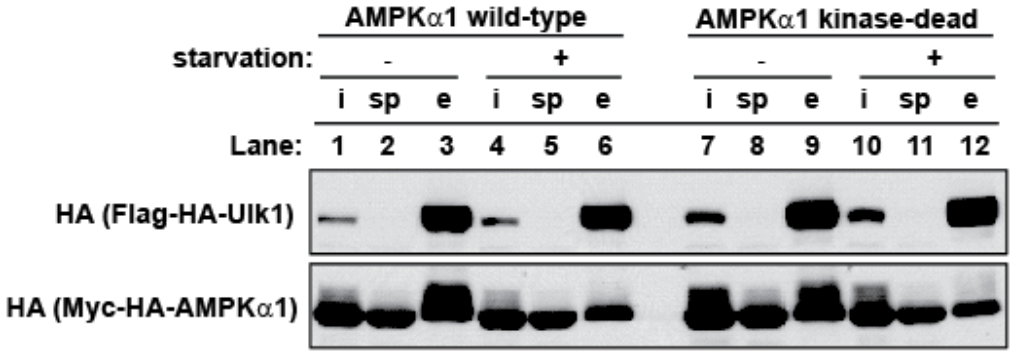

Figure III-4

Kinase activity of AMPK is not required for its interaction with Ulk1. HEK 293T cells were transfected with Flag-HA-Ulk1 and Myc-HA-AMPKα1 (either wild-type or K45R kinase-dead form). Cells were treated with either rich or total starvation medium for 1 hr, and extracts were immunoprecipitated with anti-Flag beads and eluted with Flag peptide. Association pattern between Ulk1 and AMPK remained regardless of kinase activity of AMPK. i: input; sp: soup; e: eluate.

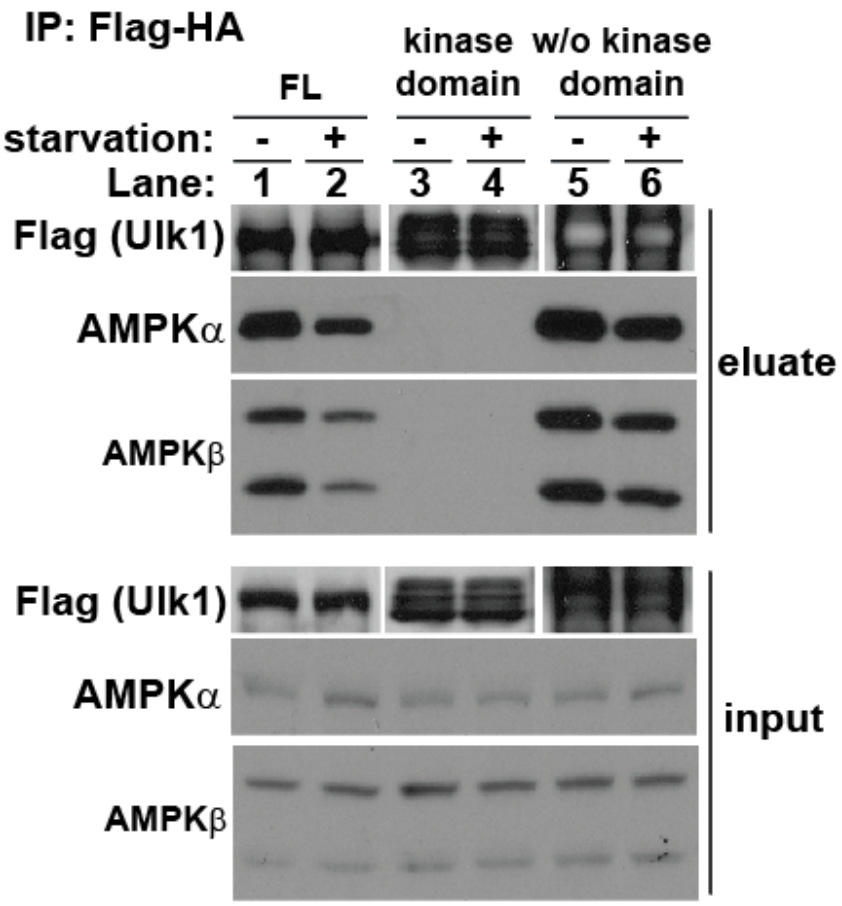

Figure III-5

AMPK interacts with Ulk1 at the region other than Ulk1's N-terminal kinase domain. HEK 293T cells were transfected with either full length Ulk1, Ulk1 kinase domain only (aa1 - aa278), or kinase-domain-deleted Ulk1 (aa279 – C-terminal end). All Ulk1 constructs are Flag-tagged at N-terminus. Cell extracts were immunoprecipitated with anti-Flag beads and eluted with Flag peptide.

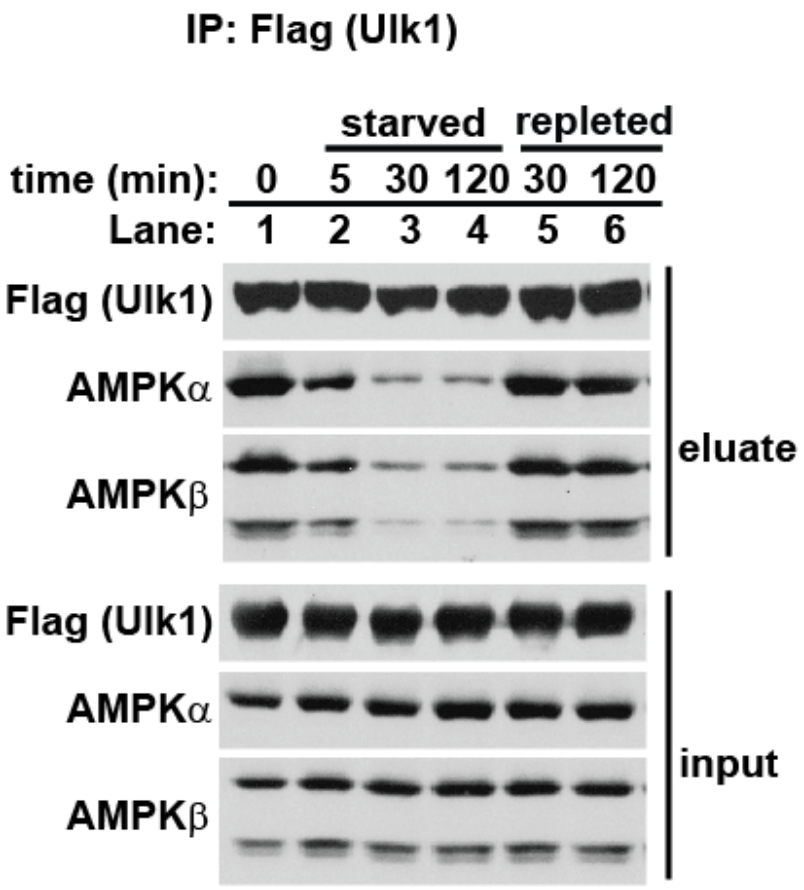

Figure III-6

Dynamics of Ulk1/AMPK interaction in response to nutrient availability. Cells were starved and repleted with rich medium for durations as indicated. Flag IP assays were then performed. Ulk1/AMPK association pattern were analyzed by Western blotting.

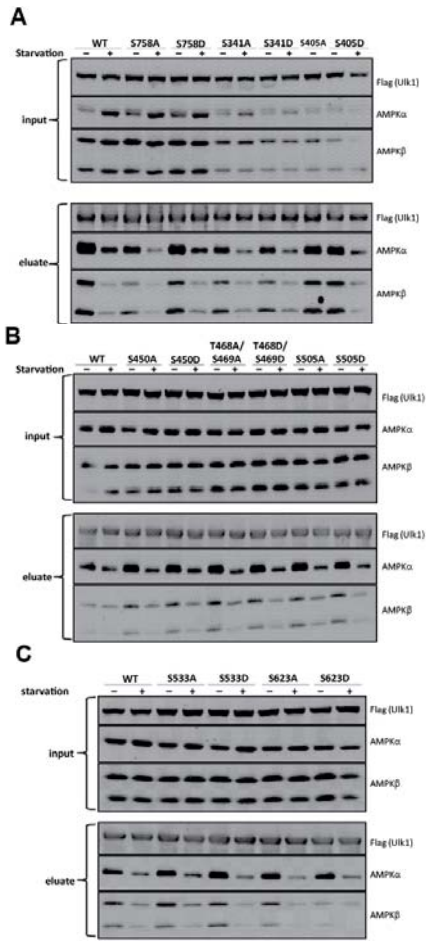

Figure III-7

Only serine 758 was identified in search of crucial phosphorylation residues of Ulk1 that are important for Ulk1/AMPK interaction. Candidate phosphorylation sites of Ulk1 were identified by SILAC and listed in Table 1. HEK 293T cells were transfected with either wild-type Flag-Ulk1 or Flag-Ulk1 phosphorylation mutants as indicated, and treated for 2 hrs with either rich or total starvation medium. Cell extracts were immunoprecipitated with anti-Flag beads, and the eluates were analyzed by Western blotting. Note the apparent weak AMPK-association by Ukl1-S341A and Ulk1-S341D is due to less input of starting materials as shown in upper panel.

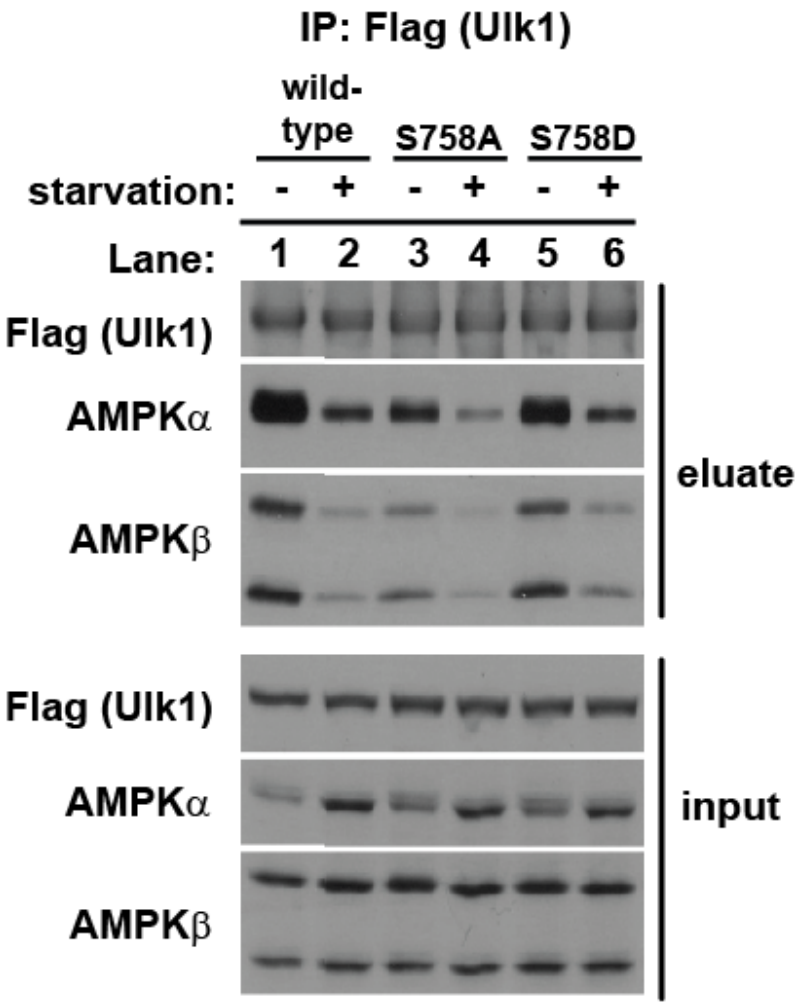

Figure III-8

Phosphorylation of Ulk1 at serine 758 was required for Ulk1/AMPK association. HEK 293T cells were transfected with either wild-type Flag-Ulk1 or Flag-Ulk1 mutants as indicated, and treated for 2 hrs in rich or total starvation medium. Cell extracts were immunoprecipitated with anti-Flag beads, and the eluates were analyzed by Western blotting.

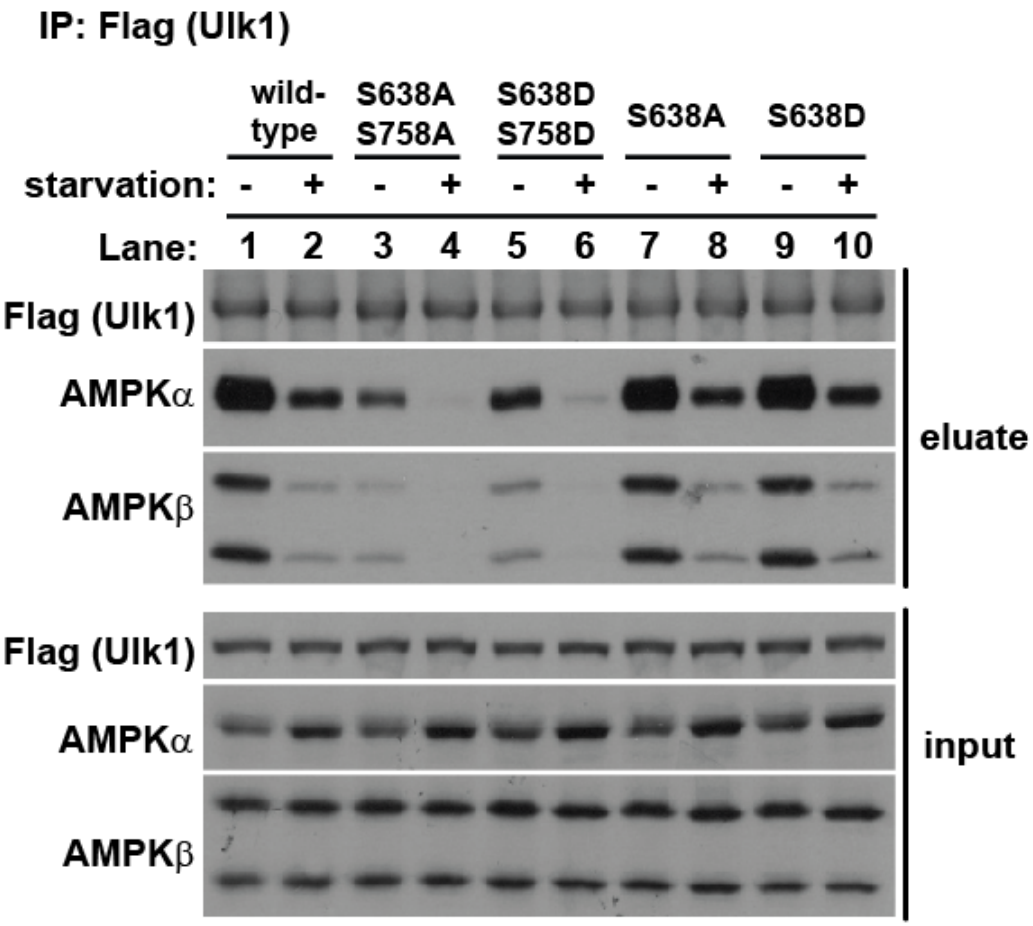

Figure III-9

Phosphorylation of Ulk1 at serine 638 was not required for Ulk1/AMPK association. Experiments were performed same as in Figure III-8 with either wild-type Ulk1 or indicated mutants. See also Figure III-7.

sequence	2/1 (of XICs) fed/starved	S.D.	sequence	2/1 (of XICs) fed/starved	S.D.
ALAGQLPAVGR	1.27	0.05	EGGVPLAPNQPVHGTQADQER	1.06	0.04
ALAGQLPAVGR	1.79	0.25	EGGVPLAPNQPVHGTQADQER	1.24	0.06
ALAGQLPAVGR	1.34	0.09	EGGVPLAPNQPVHGTQADQER	1.23	0.04
ALAGQLPAVGR	1.39	0.08	EGGVPLAPNQPVHGTQADQER	1.21	0.07
ALAGQLPAVGR	1.51	0.12	EGGVPLAPNQPVHGTQADQER	1.24	0.03
ALAGQLPAVGR	1.41	0.13	INLAFMSTR	1.42	0.08
ALAGQLPAVGR	1.20	0.03	INLAFMSTR	1.34	0.07
ALAGQLPAVGR	1.45	0.13	INLAFMSTR	1.24	0.07
ALAGQLPAVGR	1.23	0.12	INLAFMSTR	1.36	0.07
ASPHDVLETIFVR	1.16	0.15	INLAFMSTR	1.50	0.13
ASPHDVLETIFVR	1.22	0.04	INLAFMSTR	1.35	0.23
ASPHDVLETIFVR	1.17	0.02	INLAFMSTR	1.25	0.00
ASPHDVLETIFVR	1.24	0.04	INLAFMSTR	1.32	0.06
ASPHDVLETIFVR	1.25	0.07	INLAFMSTR	1.50	0.05
ASPHDVLETIFVR	1.35	0.02	INLAFMSTR	1.44	0.10
ASPHDVLETIFVR	1.27	0.03	INLAFMSTR	1.25	0.12
ASPHDVLETIFVR	1.25	0.07	INLAFMSTR	1.36	0.13
ASPHDVLETIFVR	1.25	0.02	INLAFMSTR	1.27	0.05
ASPHDVLETIFVR	1.07	0.07	INLAFMSTR	1.22	0.17
ApSPHDVLETIFVR	**1.42**	**0.84**	INLAFMSTR	1.51	0.06
ApSPHDVLETIFVR	**1.43**	**0.00**	INLAFMSTR	1.40	0.06
ASPHDVLETIFVRK	1.43	0.06	IYFGEVQLSGLGEGFQTVR	1.33	0.00
DDILPMDLGTFYR	1.35	0.00	IYFGEVQLSGLGEGFQTVR	1.22	0.00
DDILPMDLGTFYR	1.41	0.00	IYFGEVQLSGLGEGFQTVR	1.39	0.06
DDILPMDLGTFYR	1.08	0.00	IYFGEVQLSGLGEGFQTVR	1.38	0.08
DDILPMDLGTFYR	1.29	0.00	IYFGEVQLSGLGEGFQTVR	1.31	0.08
DDILPMDLGTFYR	1.36	0.00	IYFGEVQLSGLGEGFQTVR	1.45	0.07
DDILPMDLGTFYR	1.38	0.37	IYFGEVQLSGLGEGFQTVR	1.42	0.09
DIPEVTHEAK	1.24	0.11	KALAGQLPAVGR	1.44	0.13
DIPEVTHEAK	1.44	0.13	KQGHEYVILYR	1.35	0.08
DIPEVTHEAK	1.40	0.09	KQGHEYVILYR	1.34	0.08
DIPEVTHEAK	1.37	0.14	KQGHEYVILYR	1.27	0.15
DIPEVTHEAK	1.44	0.02	KQGHEYVILYR	1.53	0.05
DIPEVTHEAKK	1.45	0.08	KQGHEYVILYR	1.38	0.04
DIPEVTHEAKK	1.45	0.07	KQGHEYVILYR	1.50	0.04
DIPEVTHEAKK	1.64	0.09	KQGHEYVILYR	1.39	0.05
DIPEVTHEAKK	1.28	0.14	KQGHEYVILYR	1.44	0.08
DIPEVTHEAKK	1.24	0.08	KQGHEYVILYR	1.34	0.13
DLDKFIK	1.16	0.10	KQGHEYVILYR	1.32	0.04
DLDKFIK	1.65	0.00	KVGAFVNKPINQVTLTSLDIPFAM	1.46	0.23

Table III-1

Phosphorylation level of mAtg13 did not respond promptly to nutrient availability. Quantification of Atg13 phosphorylation is listed. Phosphorylated residues and quantitative changes of phosphorylation level of Ulk1 were identified by SILAC. Only 1 phospho-peptide (ApSPHDVLETIFVR) was identified.

sequence	2/1 (of XICs) fed/starved	S.D.
QGHEYVILYR	1.42	0.07
QGHEYVILYR	1.18	0.09
QGHEYVILYR	1.36	0.00
QGHEYVILYR	1.53	0.07
QGHEYVILYR	1.41	0.05
SMCVEISLK	1.41	0.10
SMCVEISLK	1.41	0.08
SMCVEISLK	1.28	0.07
SMCVEISLK	1.51	0.09
SSSSPTGSDWFNLAIK	1.26	0.13
SSSSPTGSDWFNLAIK	1.43	0.06
SSSSPTGSDWFNLAIK	1.46	0.00
SSSSPTGSDWFNLAIK	1.35	0.05
SSSSPTGSDWFNLAIK	1.31	0.08
SSSSPTGSDWFNLAIK	1.38	0.06
SSSSPTGSDWFNLAIK	1.28	0.20
SSSSPTGSDWFNLAIK	1.34	0.06
SSSSPTGSDWFNLAIK	1.29	0.00
SSSSPTGSDWFNLAIK	1.31	0.06
SSSSPTGSDWFNLAIK	1.37	0.05
SSSSPTGSDWFNLAIK	1.26	0.05
SSSSPTGSDWFNLAIK	1.31	0.05
SSSSPTGSDWFNLAIK	1.03	0.11
THCAATPSSSEDTETVSNSSEGR	1.34	0.02
THCAATPSSSEDTETVSNSSEGR	1.36	0.03
THCAATPSSSEDTETVSNSSEGR	1.33	0.06
THCAATPSSSEDTETVSNSSEGR	1.34	0.01
THCAATPSSSEDTETVSNSSEGR	1.45	0.05
THCAATPSSSEDTETVSNSSEGR	1.30	0.00
THCAATPSSSEDTETVSNSSEGR	1.03	0.06
TVQVIVQAR	1.44	0.06
TVQVIVQAR	1.21	0.15
TVQVIVQAR	1.47	0.00
TVQVIVQAR	1.35	0.05
TVQVIVQAR	1.23	0.08
TVQVIVQAR	1.19	0.08
TVQVIVQAR	1.27	0.11
VGAFVNKPINQVTLTSLDIPFAMFAPK	1.43	0.00
VGTVGTPVGTITLSCAYR	1.33	0.07
VGTVGTPVGTITLSCAYR	1.33	0.13

Table III-1 cont'd

Quantification of the Ulk1 phosphorylated peptides

phospho-sites	*Phosphorylation ratio (fed/starved)	S.D.
serine 341	1.61	0.29
serine 405	0.59	0.06
serine 450	3.28	0.05
threonine 468	2.85	0.14
serine 469	1.14	0.02
serine 479	5.01	0.07
serine 505	2.15	0.04
serine 533	0.67	0.04
serine 556	6.94	0.28
serine 623	0.93	0.07
serine 638	11.55	N/A
serine 758	12.31	0.21
serine 775	3.63	0.09

*calculated from ratio of identified phospho-peptide amount, and corrected to the amount of Ulk1 non-phosphorylated backbone peptides. S.D., standard deviation.

Table III-2

Quantification of the Ulk1 phosphorylated peptides reveals that phosphorylation of Ulk1 is globally decreased after starvation. 13 Phosphorylated residues were identified. Quantitative changes of phosphorylation level were recorded by SILAC. Serine 638 and serine 758 showed more than 10 folds decrease in phosphorylation level upon starvation.

Accession Number	Protein name	Protein ratio (fed/starved)		
		Corrected to actin (0.92)	Corrected to Ulk1 (0.18)	S.D.
(Quantification of Ulk1 protein complex)				
IPI00289357	Ulk1	0.20	1.00	0.32
IPI00006080	Atg13	0.66	3.40	0.11
IPI00783392	FIP200	0.83	4.24	0.12
IPI00796677	Atg101	0.89	4.54	0.07
IPI00872459	AMPKα	3.87	19.80	0.55
IPI00219377	AMPKγ	2.90	14.83	0.40
(Quantification of Atg13 protein complex)				
IPI00006080	Atg13	1.42	1.00	0.13
IPI00289357	ULK1	1.42	1.00	0.28
IPI00783392	FIP200	1.21	0.85	0.10
IPI00305296	Atg101	1.43	1.01	0.18

Table III-3

SILAC reveals Ulk1, but not mAtg13, interacts with AMPK. Listed are major Ulk1- and mAtg13-associated proteins and quantitative change in response to nutrient availability, as identified by SILAC. HeLa Flag-HA-Ulk1 or HeLa Flag-HA-Atg13 stable cells were cultured in accordance with requirement of SILAC. Cells were then treated for 2 hrs with either rich or total starvation medium. Flag-HA tandem IP was performed. The eluted Ulk1 and Atg13 immunocomplexes were analyzed by SILAC. S.D. stands for standard deviation.

IV. REGULATION OF ULK1 PHOSPHORYLATION

Abstract

This chapter focuses on regulation of Ulk1 phosphorylation at serine 638 and serine 758. First, time course experiments were performed and I noticed that these two sites exhibit different dynamics, suggesting they are regulated differently. Therefore, I started to investigate what are the upstream kinases responsible for these two phosphorylation events. In brief, serine 638 is phosphorylated by both AMPK and mTOR, while serine 758 is phosphorylated by mTOR but not AMPK. It is not known yet whether mTOR and AMPK are the direct kinases responsible for these sites.

Introduction

Several recent studies using mammals and *Drosophila* identified a direct interaction between the mTOR and the Atg1/Ulk1 complexes. mTORC1 is highly sensitive to nutrient availability and mTORC1, but not mTORC2, is incorporated into the Ulk1 complex (Ulk1/FIP200/mAtg13/Atg101) when nutrients are abundant. This incorporation is mediated by raptor, a substrate-recognition adaptor of mTORC1. This interaction between mTORC1 and Ulk1 complex is independent of mAtg13, as a C-terminal deletion mutant of Ulk1 which is unable

to interact with mAtg13 can still bind to raptor. Both *in vitro* and *in vivo* data suggest that mTORC1 phosphorylates Ulk1 and mAtg13 under nutrient rich conditions, yet the specific residues have not been identified. Rapamycin treatment facilitates the phosphorylation of FIP200 by Ulk1, and over-expression of Rheb inhibits Ulk1 kinase activity *in vitro*. All these data suggest that mTORC1 suppresses the kinase activity of Ulk1. In *Drosophila*, dTor also interacts with dAtg1 and phosphorylates dAtg1 and dAtg13 in a nutrient-dependent manner. The detailed mechanism by which mTROC1 regulates kinase activity of Atg1 remains to be elucidated, and it is essential to identify phosphorylation sites present in Atg1 by mTORC1.

(for detailed references, please refer to Chapter 1 – INTRODUCTION)

Results and Discussions

Different nutritional signals regulate Ulk1 phosphorylation at serine 638 and serine 758

Time course experiments were performed to monitor the dynamics of phosphorylation changes at serine 638 and serine 758 in response to nutrient availability. Serine 638 was found to respond faster than serine 758. As shown in Figure IV-1, 5 minutes after medium withdrawal, serine 638 was largely

dephosphorylated. For serine 758, this process took 30 minutes. Similarly, when cells were replenished with medium, serine 638 was rapidly re-phosphorylated in 5 minutes, while it took 30 minutes for serine 758 to be phosphorylated again.

Phosphorylations at serine 638 and serine 758 exhibited different kinetics, suggesting that these two sites are regulated differently. I next investigated what are the specific nutritional triggers for phosphorylations at these two sites. As shown in Figure IV-2, DMEM (Dulbecco's modified eagle medium) withdrawal remarkably decreases phosphorylation at serine 638, while serum withdrawal has minor effects on this residue. Nevertheless, ULK1 protein was downshifted. In contrast, phosphorylation at serine 758 was severely affected by either serum or DMEM withdrawal.

Each component from DMEM was further screened for its role in ULK1 phosphorylation (for DMEM formula, see Table IV-1). Unexpectedly, among all components in DMEM, calcium showed the biggest effect on serine 638 phosphorylation. Simply adding calcium to total starvation medium largely restored phosphorylation of Ulk1 at this site (Figure IV-3, compare lane 3 with lane 2). Single calcium drop-out from DMEM led to dephosphorylation at serine 638, but not to the same extent as in total starvation medium. These results

suggest that calcium is critical for proper phosphorylation of Ulk1 at serine 638, yet there are other nutritional factors in DMEM which also contribute. In contrast, phosphorylation of Ulk1 at serine 758 is not influenced by calcium availability.

mTOR is responsible for phosphorylation of Ulk1 at both serine 638 and 758, while AMPK is responsible for that at serine 638 only

The fact that both serine 638 and serine 758 are regulated by multiple nutrients made me suspect the involvement of mTOR kinase, which can integrate various nutritional signals and has been reported to interact with Ulk1. Indeed, rapamycin treatment induced rapid dephosphorylation at serine 638 and serine 758. Both sites started to be dephosphorylated 10 minutes after treatment (Figure IV-4). Furthermore, knockdown of mTOR also led to dephosphorylation at these two sites (Figure IV-5). I conclude that mTOR signaling is required for phosphorylations at both serine 638 and serine 758 of Ulk1.

Calcium signal only affects phosphorylation at serine 638, suggesting that this residue is also under regulation of other kinase(s) besides mTOR. I noticed that knockdown of either AMPKα1/α2 or AMPKβ1/β2 subunits led to

dephosphorylation at serine 638 but not at serine 758 (Figure IV-6). Moreover, under any nutrient condition tested, there is a fine correlation between serine 638 phosphorylation and the kinase activity of AMPK as indicated by the phosphorylation at threonine 172 of AMPKα, and at serine 79 of acetyl-CoA carboxylase (ACC), a well-studied AMPK substrate (Figure IV-7). Taken together, these results indicate that besides mTOR, AMPK signaling is also required for the phosphorylation of Ulk1 at serine 638.

Experimental Procedures

Stable cell lines for inducible knockdown in U2OS cells

Detailed procedure has been described in Chapter 2. siRNA sequences used in this research were described as follows:

AMPKα1: CCCAGAGGTAGATATATG

AMPKα2: CGACTAAGCCCAAATCTTT

AMPKβ1: GTACGTCACCACCTTGTTA

AMPKβ2: GCACCAAGATTCCACTGAT

Cell culture and preparation of conditional/dropout media

All cells used in this study were cultured in Dulbecco's modified eagle medium (DMEM) supplemented with 10% regular FBS or dialyzed FBS, 200ug/ml penicillin and 100ug/ml streptomycin, referred to as "rich medium". Unless indicated otherwise, cells were starved in Hank's buffered salt solution (HBSS, without calcium/magnesium) containing 1% regular medium (for better cell adherence), referred to as "total starvation medium". Each ingredient from DMEM was prepared as stock solution and conditional/dropout DMEM media were reconstituted from these stocks with omission of indicated ingredient(s). All chemicals used for preparation of drop-out media were from Sigma.

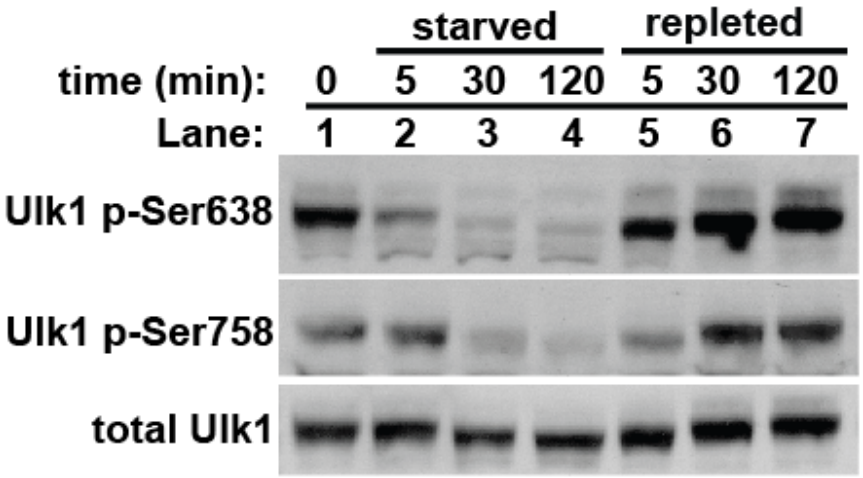

Figure IV-1

Dynamics of Ulk1 phosphorylation. U2OS cells were starved in total starvation medium (HBSS solution containing 1% rich medium), and then replenished with rich medium (DMEM plus 10% dialyzed FBS) for durations as indicated. Cell extracts were analyzed by Western blotting to visualize phosphorylations of Ulk1 at serine 638 and serine 758.

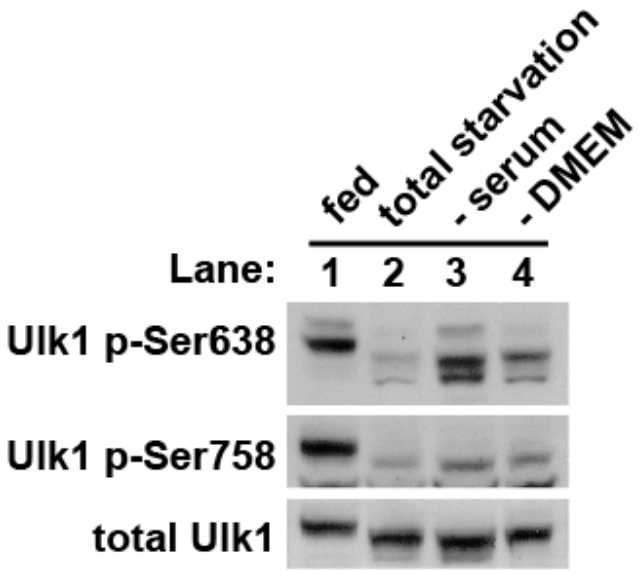

Figure IV-2

U2OS cells were treated for 2 hr as indicated. For serum withdrawal, cells were cultured in DMEM without fetal bovine serum (FBS); for DMEM withdrawal, cells were cultured using 10% dialyzed FBS in HBSS (Hank's balanced salt solution). Phosphorylations of Ulk1 at Ser638 and Ser758 were analyzed using phospho-specific antibodies against these two sites.

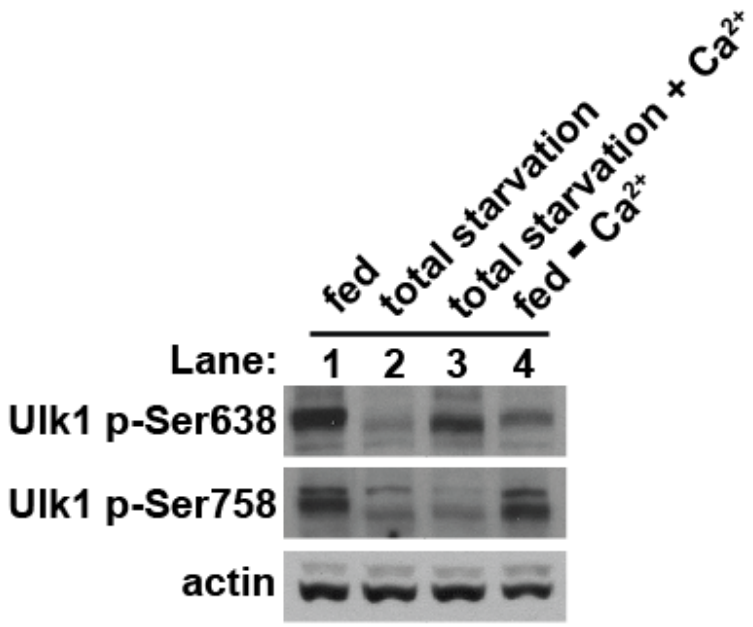

Figure IV-3

Calcium is crucial for phosphorylation of Ulk1 at serine 638, but not serine 758. U2OS cells are treated for 2 hr as indicated. Lane 3: calcium was added into total starvation medium to reach the same calcium concentration as in regular DMEM (0.2 g/L); Lane 4: regular DMEM medium (containing 10% dialyzed FBS) with single drop-out of calcium.

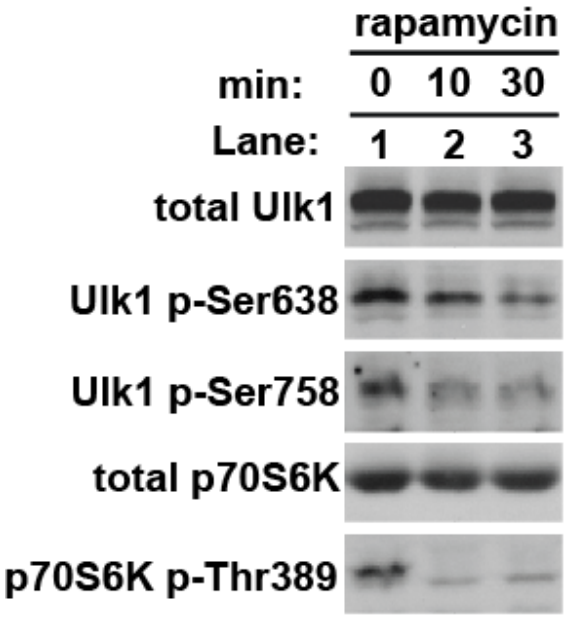

Figure IV-4

Rapamycin treatment induced dephosphorylation of Ulk1 at both serine 638 and serine 758. U2OS cells were cultured in rich medium and rapamycin was added. Cells were then collected at given time points after rapamycin treatment.

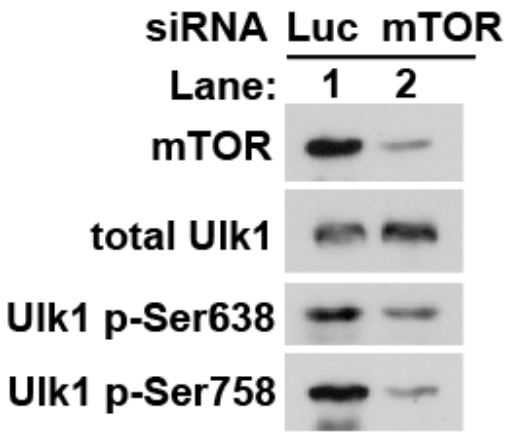

Figure IV-5

Knockdown of mTOR induced dephosphorylation of Ukl1 at both serine 638 and serine 758. U2OS cells were transfected with either control siRNA (Luc) or mTOR siRNA oligos. 72 hrs after transfection, cells were collected and extracts analyzed by Western blotting.

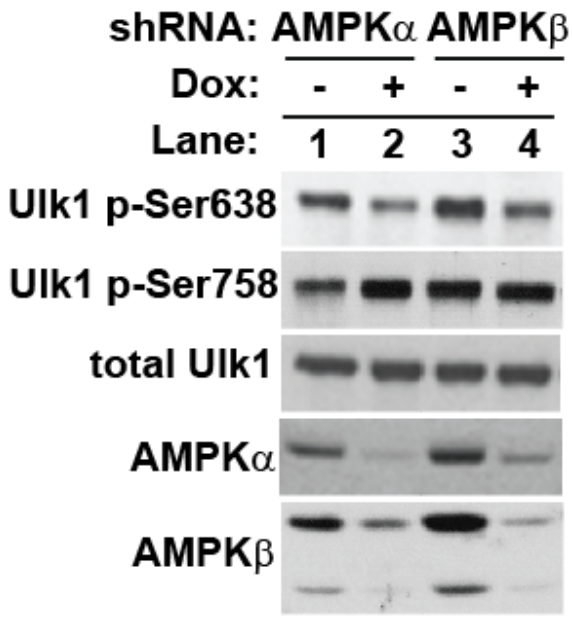

Figure IV-6

Knockdown of AMPK induced dephosphorylation of Ulk1 at serine 638, but not serine 758. U2OS stable cell lines that inducibly knock down AMPKα (α1 & α2) or AMPKβ (β1 & β2) upon addition of doxycycline (Dox) were generated. 72 hrs after addition of Dox, phosphorylations of Ulk1 at Ser638 and Ser758 were visualized by Western blotting.

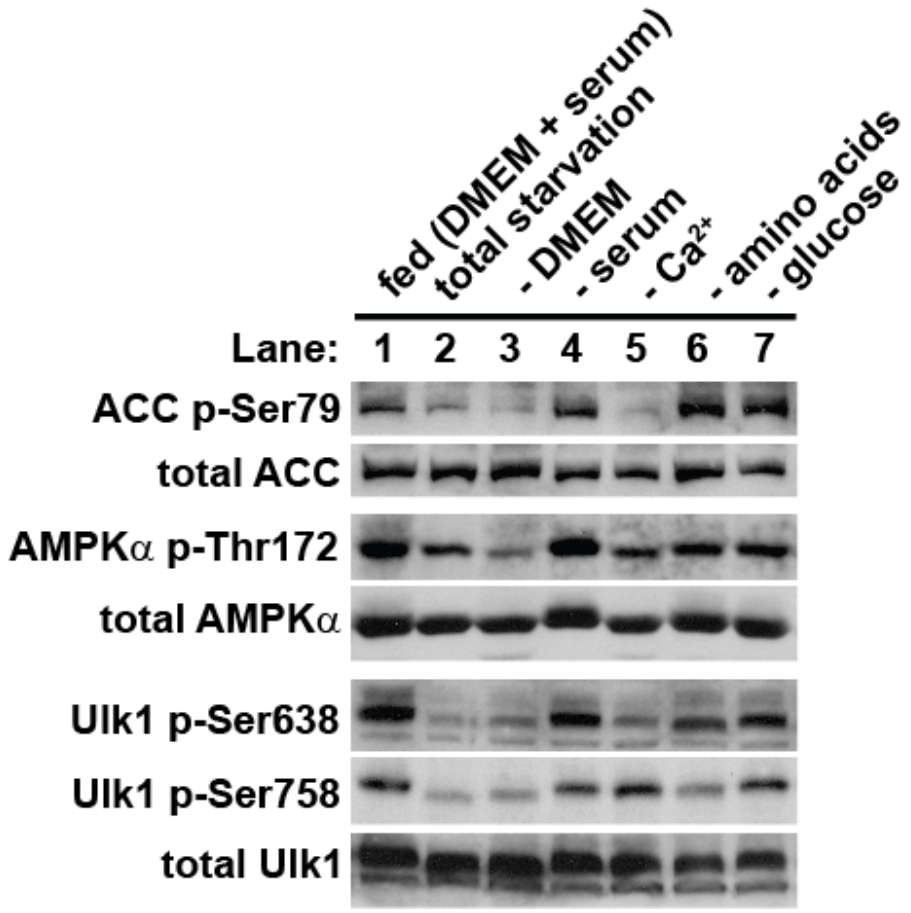

Figure IV-7

AMPK activity correlates with phosphorylation of Ulk1 at serine 638 but not serine 758 in response to various nutrient conditions. U2OS cells were treated for 2 hr as indicated and cell extracts were analyzed by Western blotting.

COMPONENTS	MW	Conc (mg/L)
Amino Acids		
L-Arginine hydrochloride	211	84
L-Cystine 2HCl	313	62.6
L-Glutamine	146	584
Glycine	75	30
L-Histidine hydrochloride-H2O	210	42
L-Isoleucine	131	105
L-Leucine	131	105
L-Lysine hydrochloride	183	146
L-Methionine	149	30
L-Phenylalanine	165	66
L-Serine	105	42
L-Threonine	119	95
L-Tryptophan	204	16
L-Tyrosine disodium salt dihydrate	225	89.5
L-Valine	117	94

COMPONENTS	MW	Conc (mg/L)
Vitamins		
Choline chloride	140	4
Folic Acid	441	4
myo-Inositol	180	7.2
Nicotinamide	122	4
D-pantothenic Acid (hemicalcium)	238.27	4
Pyridoxine hydrochloride	206	4
Riboflavin	376	0.4
Thiamine hydrochloride	337	4

COMPONENTS	MW	Conc (mg/L)
Inorganic Salts		
Calcium Chloride ($CaCl_2 \cdot 2H_2O$)	147	264.9
Ferric Nitrate ($Fe(NO_3)_3 \cdot 9H_2O$)	404	0.1
Magnesium Sulfate ($MgSO_4$)	120	97.7
Potassium Chloride (KCl)	75	400
($NaH_2PO_4 \cdot H_2O$)	138	125
Sodium Bicarbonate (NaHCO3)	84	1500
Sodium Chloride (NaCl)	58	6400

COMPONENTS	MW	Conc (mg/L)
Other Components		
D-Glucose (Dextrose)	180	4500
Phenol Red	376.4	15
Sodium Pyruvate	110	110

Table IV-1

Components, concentration, and classification of DMEM.

V. FUNCTIONAL OUTPUT OF ULK1/AMPK INTERACTION

Abstract

In this chapter, by comparison between wild-type Ulk1 and the Ulk1 S758A mutant that fails to interact with AMPK properly, I started to investigate whether Ulk1 phosphorylation and subsequent Ulk1/AMPK interaction have any impact toward autophagy. Three different approaches were adopted to monitor autophagy and the results are consistent with each other.

In brief, I assayed for long-lived protein degradation rate, hVPS34 activity, and LC3II/LC3I conversion. All data indicate that, upon starvation, the Ulk1 S758A mutant induces autophagy much faster compared to the wild-type Ulk1. This mutant does not alter the maximum capacity of autophagy, as prolonged starvation shows no difference in autophagy induction between wild-type Ulk1 and the mutant.

Introduction

Macroautophagy is a three-step process: (1) autophagosomes form and mature, (2) the autophagosomes fuse with lysosomes, and (3) the autophagic cargo is degraded in the lysosomes. It is this lysosomal degradation of the

autophagic cargo that constitutes the autophagic flux. As in the case of metabolic pathways, the steady-state concentration of the intermediary autophagic structures alone is insufficient for investigating the flux. Assaying the degradation of long-lived proteins as described in this chapter is one of the methods that can be used to measure autophagic flux.

Functional outputs of autophagy are generally considered as accumulative and relatively slow processes. A variety of assays monitor autophagic readouts in wide time windows, normally hours after treatments that perturb cellular signalings. Yet, upstream regulations of autophagy occur mainly through kinase cascades that are inherently prompt. It is therefore conceptually plausible that autophagy can be detected at earlier time points, especially when cultured cells are treated with harsh conditions such as total medium/serum withdrawal.

(for detailed references, please refer to Chapter 1 – INTRODUCTION)

Results and Discussions

Wild-type Ulk1 and Ulk1 S758A mutant show no difference in autophagy induction when mAtg13 is present

Both SILAC and western blotting data show that AMPK associates with Ulk1 but not mAtg13. A recent study also reported that various AMPK subunits are able to interact with mammalian autophagy initiating factors such as Ulk1/2, FIP200 and Atg101, but not mAtg13 (Behrends et al., 2010). These observations raise the possibility that Ulk1 may exist in two mutually exclusive complexes: both will have core components such as Ulk1/2, FIP200 and Atg101, and either mAtg13 or AMPK bound to these core factors. Both may contribute to autophagy induction and it is therefore difficult to characterize the functional outputs from one particular complex in the presence of the other. Indeed, for autophagy level as tested by long-lived protein degradation (LLPD) assay, no significant difference was observed between wild-type Ulk1 and the S758A mutant defective in AMPK association (Figure V-1).

Ulk1 S758A mutant induces autophagy faster compared to wild-type Ulk1 when mAtg13 is absent

I tried to resolve this issue by knocking down mAtg13 and therefore eliminating the activity generated from the mAtg13 complex. Interestingly, absence of mAtg13 led to dramatic Ulk1 destabilization (Figure V-2; also see in Hosokawa et al., 2009a). I then used this cellular background (absence of both Ulk1 and mAtg13) to study the Ulk1/AMPK interaction, and performed rescue experiments with either wild-type Ulk1 or Ulk1-S758A mutant. Autophagy is dampened if the protein level of mAtg13 and/or Ulk1 is decreased. Nonetheless, LLPD assay showed that, in the absence of mAtg13, autophagy could still be greatly induced when cells were starved. In the first 10 minutes during starvation, U2OS cells expressing Ulk1-S758A mutant induced much more protein degradation than those expressing wild-type Ulk1 (Figure V-3). 30 minutes after starvation, the mutant still exhibited more than 20% excess of activity compared to the wild-type (Figure V-4A). This difference in LLPD between wild-type Ulk1 and S758A mutant disappeared after prolonged starvation for 120 minutes (Figure V-4B). These results correlate with the dynamics between Ulk1 and AMPK interaction, as it takes about 30 min of starvation for wild-type Ulk1 to dissociate with AMPK. After that time point, wild-type Ulk1 should behave

similar to the mutant in terms of AMPK-association pattern and consequent functional outputs.

The Class III PI3K, hVps34, phosphorylates the inositol ring of phosphatidylinositol (PI) at the D3 position to generate PI3P, a step essential for autophagosome formation. The hVps34 proteins from cells expressing Ulk1-S758A mutant has higher in vitro activity compared those from cells expressing wild-type Ulk1 protein under fed condition (Figure V-5). This indicates the Ulk1 mutant defective in AMPK association may better prime cells for autophagy induction with higher Class III PI3K activity. Upon starvation, the PI3K activity of hVps34 further increased, yet differences between the wild-type and the mutant became less obvious as starvation prolonged (Table V-1).

Taken together, these data shows that the Ulk1-S758A mutant defective in Ulk1/AMPK interaction initiates starvation-induced autophagy faster at early time points, but does not change the maximum capacity.

Proper phosphorylation at serine 638 facilitates phosphorylation at serine 758 and proper Ulk1/AMPK association

Alteration in serine 638, the other most regulated residue besides serine 758, does not affect the apparent Ulk1/AMPK association. Consequently, it is

difficult to observe the functional impacts of serine 638 phosphorylation toward autophagy using LLPD or other assays. Instead, since serine 638 always responds to nutrient signals faster compared to serine 758 as shown in Figure 1A, I asked whether phosphorylation at serine 638 facilitates such change at serine 758. The experiment was carried out in U2OS cells in which endogenous Ulk1 was stably knocked down. The cells were then rescued with either wild-type Ulk1 or Ulk1-S638A mutant. No obvious difference was observed between the wild-type and the mutant in terms of dephosphorylation rate at serine 758 upon starvation (Figure V-6). However, when cells were replenished with rich medium, rephosphorylation at serine 758 was much stronger in the wild-type background compared to that in the S638A mutation background. This result indicates that proper phosphorylation at serine 638 promotes faster recovery of phosphorylation at serine 758 (Figure V-6, compare lane 9,10 with lane 4,5), therefore may facilitate faster re-association between Ulk1 and AMPK when nutrients are repleted.

Experimental Procedures

Phosphatidylinositol 3-Phosphate (PI3P) quantification (ELISA for hVps34 activity)

For detail, refer to the protocol for class III PI3-Kinase kit (96-well ELISA assay for detection of PI3P) by Echelon Inc (cat# K-3000). In brief, endogenous hVps34 proteins were immunoprecipitated and incubated with PI substrate for 2 hrs to catalyze the synthesis of PI3P. The reaction (containing synthesized PI3P product) was then added to 96-well coated with PI3P. Detector proteins that recognize PI3P were also added to the wells. In the next 2 hrs, the PI3P immobilized on the 96-well plate competed with free PI3P in the reaction for detector binding. The amount of detector proteins bound to the plate is determined through colorimetric detection at 450 nm absorbance. The reading was inversely proportional to the amount of PI3P produced by hVps34.

Generation of wild-type and mAtg13 knockout MEF cells

mAtg13 knockout mice were generated by deleting the exon 2-5 and making reading frame shift beyond. Positive ES clones were injected into blastocyst isolated from C57. Germline transmission was identified by Southblot and PCR.

To generate MEF cells, aseptically dissect mouse embryos at E12.5-15.5 dpc from one pregnant mouse. Place the embryos in a 10-cm dish containing PBS. Take York sac into 1.5 ml tube for genotyping. Remove embryo's limbs, upper part of the head and discard the internal organs. Rinse the carcasses three times in a 10cm dish containing PBS. Mince the embryos into very small pieces with a sterile surgical blade. Transfer the minced embryos into a 15-ml tube containing 2ml 0.25% trypsin/EDTA and incubate at 37 ^{o}C for 20 min with shaking. Add 2ml trypsin/EDTA and incubate at 37 ^{o}C for another 20min with shaking; repeat twice. Add 6ml DMEM containing 10% FBS and pipette 20 times. Sit 5 min to allow undigested tissues down to bottom. Transfer the cell suspension into a new 15ml tube. Centrifuge at 200 g for 5 min and resuspend the pellet with MEF media. Resuspend cells with 10ml MEF media and plate onto 25cm T-flask. Change medium next day.

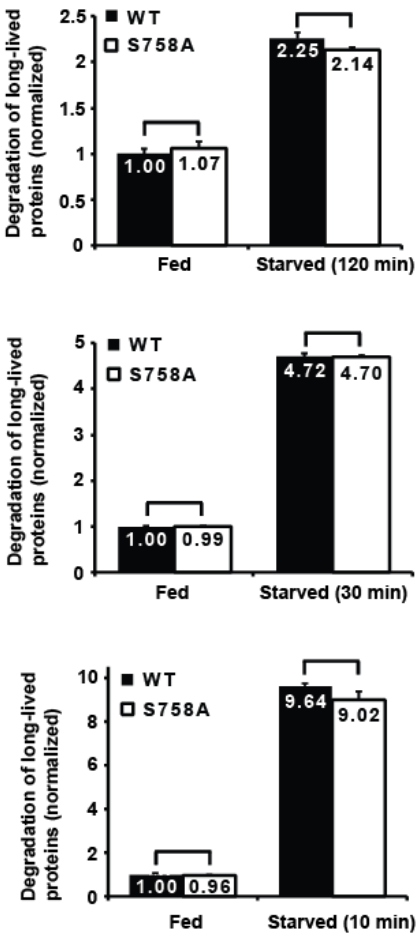

Figure V-1

Long-lived protein degradation (LLPD) assay showed in the presence of mAtg13, no difference was observed between wild-type Ulk1 and Ulk1-S758A mutant. U2OS stable cell line that inducibly knock down Ulk1 upon addition of doxycycline (Dox) was generated. 72 hrs after addition of Dox, cells were transfected with either wild-type Ulk1 of Ulk1-S758A construct, and cultured for another 48 hrs in rich medium containing no ^{3}H-labelled but excessive cold leucine. Cells were than cultured in either rich or total starvation medium for durations as indicated. A: 120 min; B: 30 min; C: 10 min. Percentages of ^{3}H-labelled leucine released into medium were calculated.

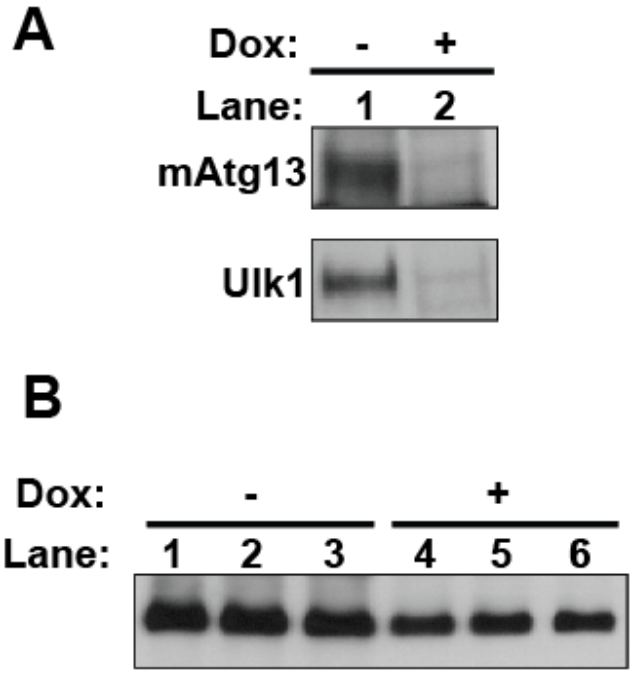

Figure V-2

(A) Knockdown of mAtg13 led to absence of Ulk1. U2OS stable cell line that inducibly knock down mAtg13 upon addition of doxycycline (Dox) was generated. 72 hrs after Dox treatment, cell extracts were analyzed by Western blotting. (B) Same as in (A), mAtg13-knockdown U2OS cells were transfected with Flag-tagged Ulk1 constructs. Compared to cells without mAtg13 knockdown (without Dox treatment), knockdown of mAtg13 destabilized exogenously-expressed Ulk1. Lane 1&4: wild-type Flag-Ulk1; lane 2&5: Flag-Ulk1-S758A; lane 3&6: Flag-Ulk1-S638A.

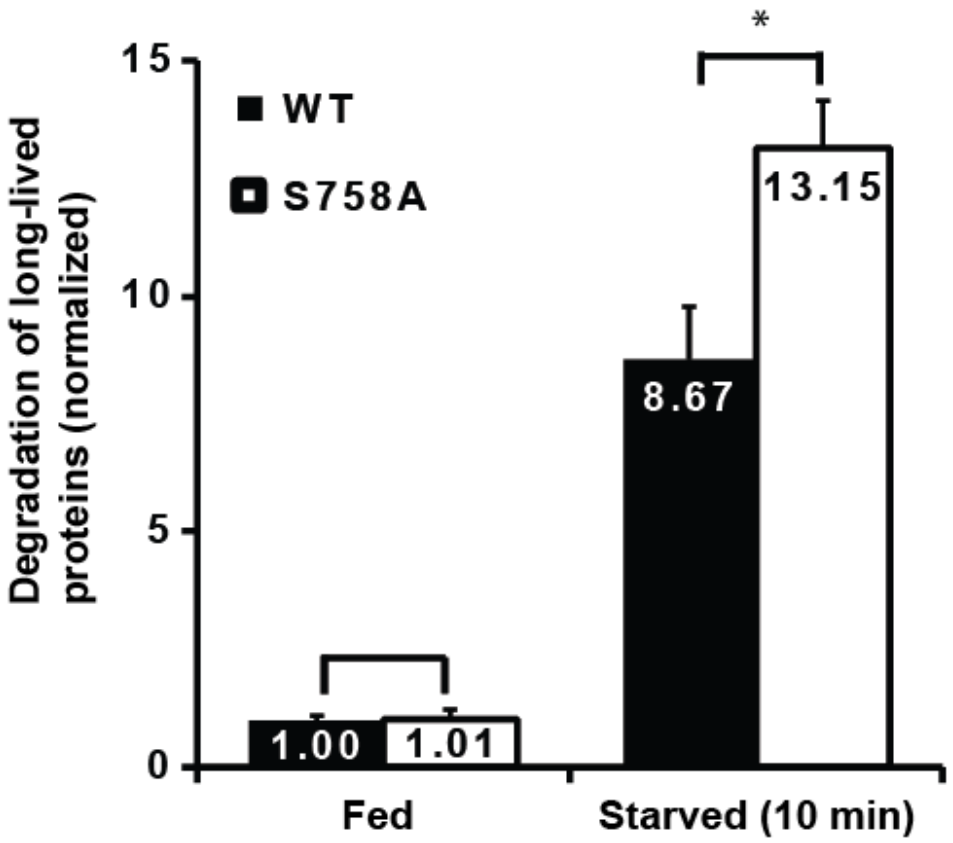

Figure V-3

Long-lived protein degradation (LLPD) assays showed Ulk1-S758A initiates starvation-induced autophagy faster compared to wild-type Ulk1 (*P = 0.003 in one-tailed Student's t-test with equal variances, n = 3). Error bar represents S.D. U2OS stable cell line that inducibly knock down mAtg13 upon addition of doxycycline (Dox) was generated. Absence of mAtg13 also led to absence of Ulk1. 72 hrs after addition of Dox, cells were transfected with either wild-type Ulk1 of Ulk1-S758A construct, and cultured for another 48 hrs in rich medium containing no ^{3}H-labelled but excessive cold leucine. Cells were than cultured in either rich or total starvation medium for 10 min. Percentages of ^{3}H-labelled leucine released from cells into medium were calculated.

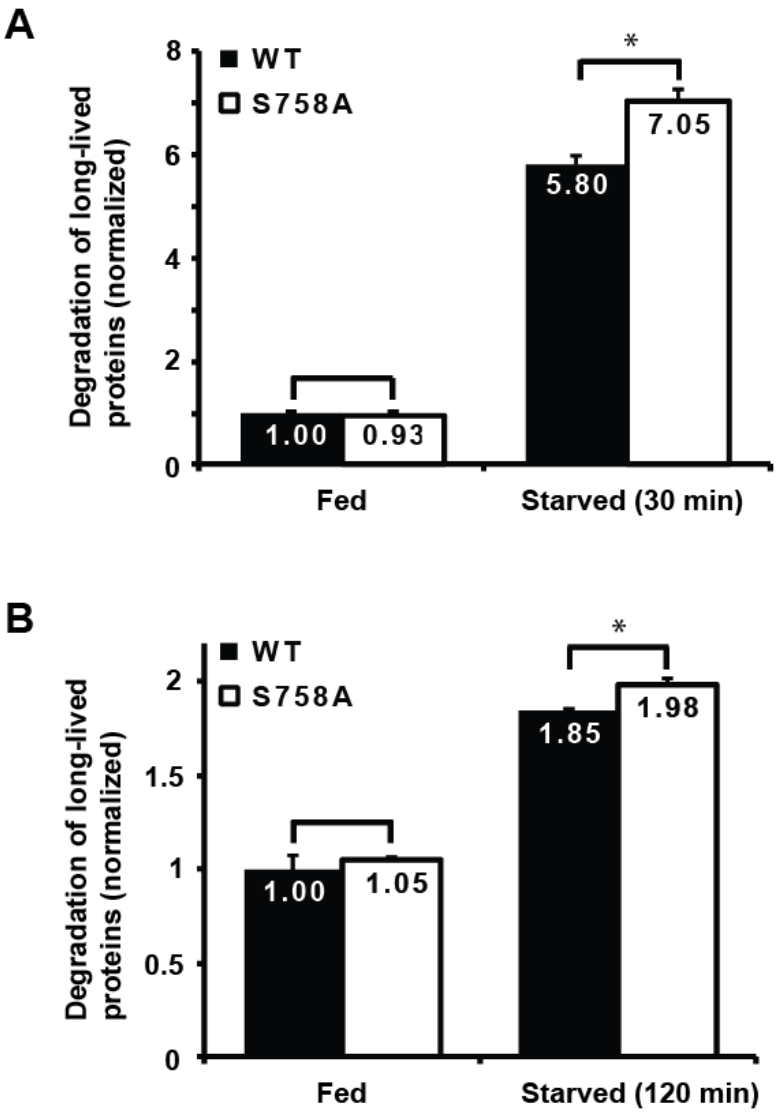

Figure V-4

Long-lived protein degradation (LLPD) assay showed in the absence of mAtg13, Ulk1-S758A mutant initiated starvation-induced autophagy faster, but gradually became similar as starvation prolonged. Experiments were performed similarly as in Fig. 4A. (G) 30 min after starvation, cells expressing Ulk1-S758A showed more LLPD. (H) 120 min after starvation, cells expressing Ulk1-S758A showed similar LLPD as the wild-type.

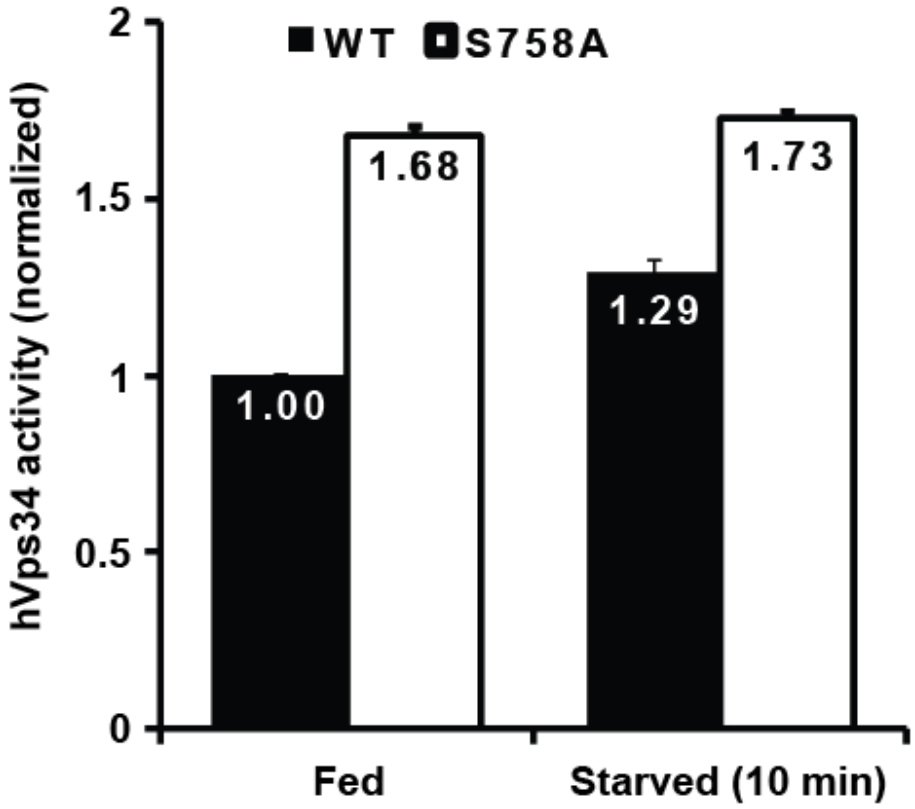

Figure V-5

In either fed condition or 10 min after starvation, cells expressing Ulk1-S758A exhibited higher hVps34 activity compared to the wild-type. Using same cells and same transfections as in (A), kinase activity of hVps34 was assayed by quantifying conversion from PI to PI3P in given time as described in Materials and Methods. Error bar represents S.D.

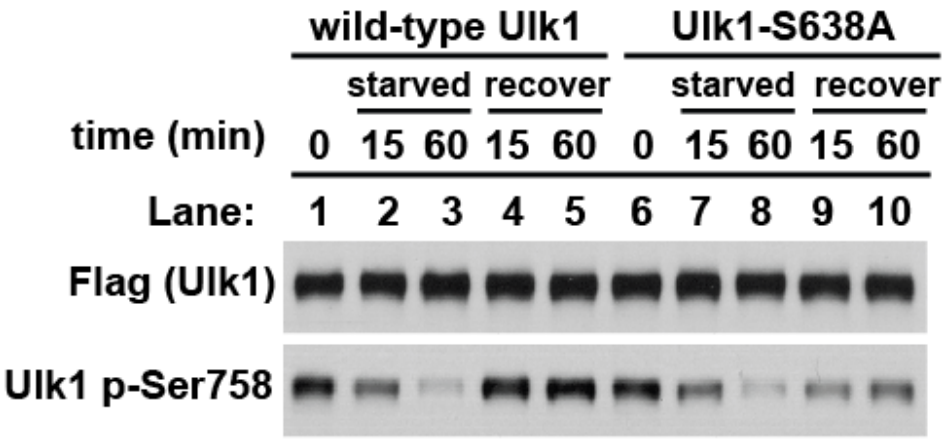

Figure V-6

In Ulk1-S638A background, serine 758 could not be properly re-phosphorylated 60 min after medium replenishment, while in wild-type Ulk1 background this process took less than 15 min. U2OS stable cell line that inducibly knock down Ulk1 upon addition of Dox was generated. 72 hrs after addition of Dox, cells were transfected with either wild-type Ulk1 of Ulk1-S638A construct, and cultured for another 48 hrs in rich medium to allow expression. Cells were then treated as indicated.

		exp#1	exp#2	exp#3	mean	S.D.
WT	0 min	1.000515	1.008369	0.991116	1	0.008638
	10 min	1.325106	1.25264	1.299069	1.292271	0.036708
	30 min	1.273431	1.287509	1.329476	1.296805	0.029156
	60 min	1.0216	1.072945	1.026692	1.040412	0.028289
S758A	0 min	1.709214	1.650494	1.677139	1.678949	0.029402
	10 min	1.751902	1.722758	1.717029	1.730563	0.018701
	30 min	1.270941	1.259027	1.330841	1.286937	0.038487
	60 min	1.203971	1.23146	1.240949	1.22546	0.019205

Table V-1

Differences of hVps34 activity between cells expressing wild-type Ulk1 and Ulk1-S758A mutant gradually disappeared as starvation prolonged. Time course of hVps34 activity (normalized) is listed. S.D. stands for standard deviation.

VI. CONCLUSIONS & DISCUSSION

I discovered that Ulk1 undergoes dramatic dephosphorylation upon starvation, particularly at serine 638 and serine 758. Phosphorylation of Ulk1 is regulated by mTOR and AMPK, and is crucial for Ulk1/AMPK association. Ulk1 dissociates with AMPK when cells are deprived of nutrients. A single serine-to-alanine mutation (S758A) on Ulk1 impairs the Ulk1/AMPK interaction. Upon starvation, this mutant Ulk1 induces autophagy much faster compared to the wild-type Ulk1.

Here I revealed several previously unknown regulatory steps occurring on Ulk1 during starvation-induced autophagy. As shown schematically in Figure VI-1, Ulk1 is hyper-phosphorylated at many serine/threonine residues including S638 and S758. Upon starvation, serine 638 is firstly dephosphorylated then serine 758 follows. These events lead Ulk1 to dissociate from AMPK and to become more active in autophagy induction. When cells are replenished with nutrients, mTOR is re-activated and phosphorylates Ulk1 at multiple sites such as S638 and S758. Proper phosphorylation of Ulk1 then leads to Ulk1/AMPK association. Though the kinase activity of AMPK is considered relatively low under nutrient-

rich condition, when in close proximity, AMPK may help maintain phosphorylation of Ulk1 at serine 638 and strengthen its association with Ulk1.

AMPK has basal level activity when cells are fed. It will be further activated upon amino acid starvation or glucose starvation (Figure IV-7, compare lane 6,7 with lane 1). Interestingly, calcium seems to be crucial for AMPK to properly exhibit its kinase activity. Basal AMPK activity will be further decreased if calcium is removed from rich medium (Figure IV-7, compare lane 5 with lane 1). This explains why total medium withdrawal, the harshest starvation condition, leads to lower AMPK activity, because calcium was also removed under this circumstance (Figure IV-7, compare lane 2 with lane 1). The kinase activity of AMPK may also contribute to autophagy induction besides classical AMPK-TSC1/2-mTOR signaling, as suggested recently by J W Lee et al that AMPK can lift the inhibitory effect of mTOR on Ulk1 by phosphorylating raptor, the key adaptor in mTORC1 (Lee et al., 2010). Taken together, I envision AMPK may have dual roles toward autophagy regulation: it promotes autophagy when cells are starved as previously well-documented, while suppresses autophagy when cells are fed by forming a complex with and confining portions of Ulk1.

Functional readouts of the Ulk1/AMPK interaction cannot be well detected in the presence of high "background noise" due to the existence of too much Ulk1/mAtg13 complex. I resolved this issue by knocking down mAtg13. Paradoxically, it seems that the presence of mAtg13 facilitates efficient phosphorylations of Ulk1 (Figure VI-2). Therefore knockout (or knockdown) of mAtg13 may impair the Ulk1/AMPK interaction due to less phosphorylation of Ulk1 at serine 758. This leads to a situation where presence of mAtg13 brings high background noise, while absence of mAtg13 brings less Ulk1/AMPK interaction. In either case, it is difficult to pinpoint the actual contribution of the Ulk1/AMPK interaction toward autophagy induction. Moreover, the Ulk1/AMPK interaction is promptly regulated. The rapid kinetics makes most qualitative assays unsuitable for monitoring autophagic effects caused by Ulk1/AMPK interaction. If nutrient deprivation prolongs, the differences between wild-type Ulk1 and the AMPK-association-defective Ulk1 mutant (Ulk1-S758A) gradually disappears. The time window for studying function of Ulk1/AMPK interaction is limited, only at the very early time point of a given environmental change. In my hands, it is less than 30 minutes after starvation. Fortunately, despite all these difficulties, the functional differences between wild-type and S758A mutant Ulk1

can be distinguished by using more quantitative approaches, such as long-lived protein degradation assay and ELISA for hVps34 activity.

Though autophagy is in general conserved from yeast to human (particularly in later stages including membrane expansion, autophagosome formation, fusion with lysosome and recycling), regulation of autophagy initiation in mammals is much more complicated and differs from yeast in many aspects. In this study, I try to elucidate this complexity by discovering a more rapid form of autophagy induction. For prolonged starvation, there is little difference between mutant Ulk1-S758A and the wild-type Ulk1, indicating that interaction between Ulk1/AMPK mainly responds to acute nutritional changes. This acute mechanism not only functions as prompt response to nutrient deprivation, but may also be a crucial exit strategy to effectively down-regulate autophagy when cells leave harsh environments and need to resume proper growth/proliferation. In summary, with this layer of regulation, mammalian autophagy is capable of responding to environmental changes more rapidly than previously considered.

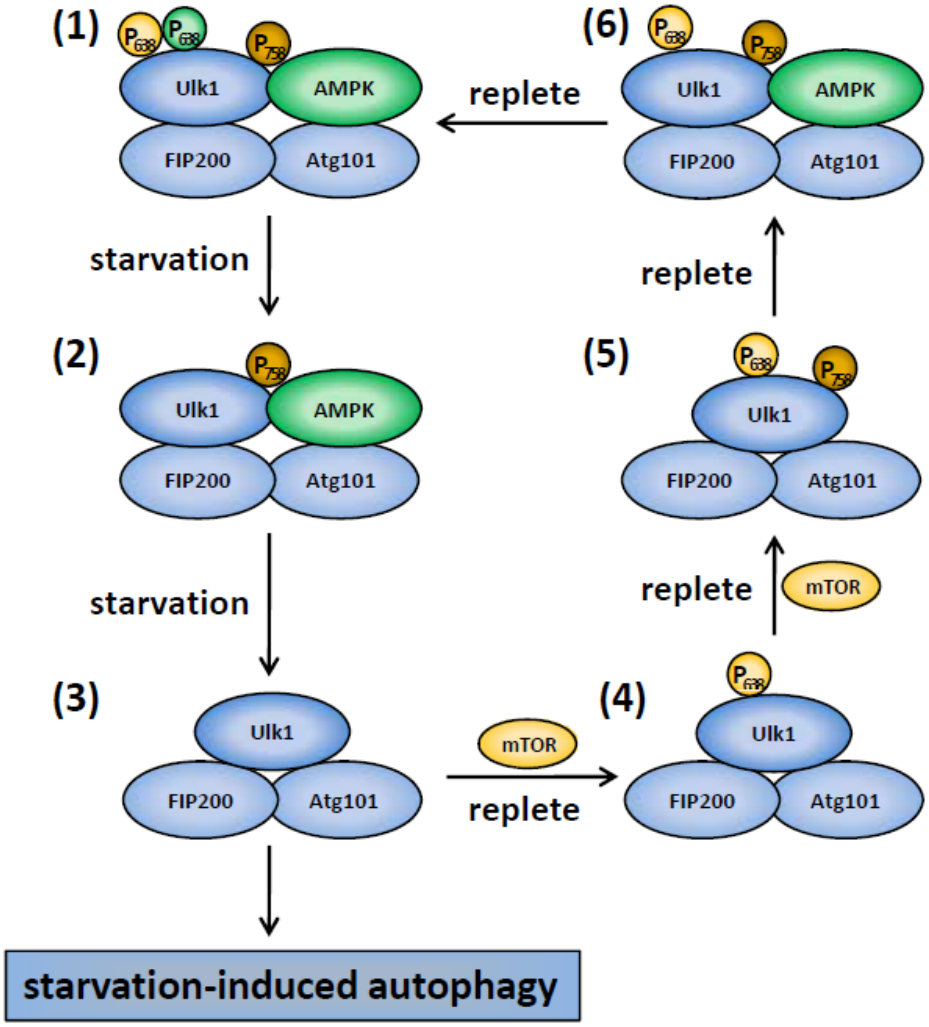

Figure VI-1

Model of Ulk1 phosphorylation in response to nutrients. When cells are fed, Ulk1 is hyper-phosphorylated at serine 638 and serine 758. About 5 - 10 min after starvation, serine 638 is dephosphorylated; 30 min after starvation, serine 758 is also dephosphorylated. Dephosphorylation of Ulk1 leads to dissociation of Ulk1/AMPK. When cells are replenished with rich medium, mTOR is activated; it phosphorylates serine 638 and serine 758. This then leads to re-association between Ulk1 and AMPK. When in close proximity, AMPK functions to maintain phosphorylation Ulk1 at serine 638.

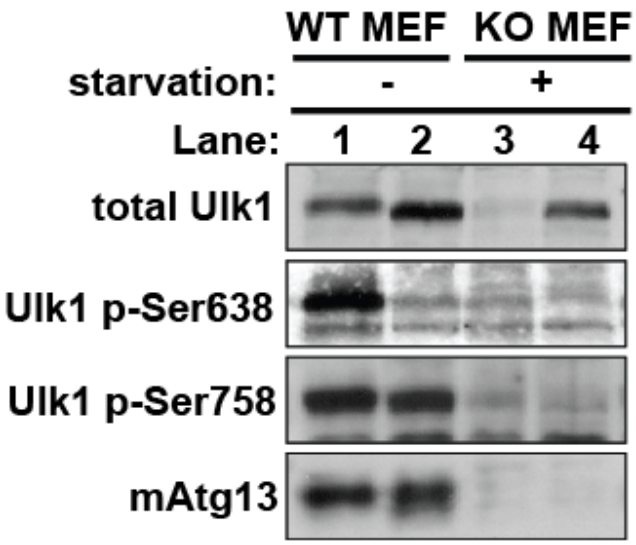

Figure VI-2

Knockout of mAtg13 impairs phosphorylations of Ulk1 at serine 638 and serine 758. Compared to wild-type (WT) MEF cells, basal Ulk1 level in mAtg13 knockout (KO) MEF cells was much lower. Both WT and KO cells increased Ulk1 protein level upon starvation.

REFERENCES

Alessi, D.R., James, S.R., Downes, C.P., Holmes, A.B., Gaffney, P.R., Reese, C.B., and Cohen, P. (1997). Characterization of a 3-phosphoinositide-dependent protein kinase which phosphorylates and activates protein kinase Balpha. Curr Biol *7*, 261-269.

Arico, S., Petiot, A., Bauvy, C., Dubbelhuis, P.F., Meijer, A.J., Codogno, P., and Ogier-Denis, E. (2001). The tumor suppressor PTEN positively regulates macroautophagy by inhibiting the phosphatidylinositol 3-kinase/protein kinase B pathway. J Biol Chem *276*, 35243-35246.

Behrends, C., Sowa, M.E., Gygi, S.P., and Harper, J.W. (2010). Network organization of the human autophagy system. Nature *466*, 68-76.

Byfield, M.P., Murray, J.T., and Backer, J.M. (2005). hVps34 is a nutrient-regulated lipid kinase required for activation of p70 S6 kinase. J Biol Chem *280*, 33076-33082.

Chan, E.Y., Longatti, A., McKnight, N.C., and Tooze, S.A. (2009). Kinase-inactivated ULK proteins inhibit autophagy via their conserved C-terminal domains using an Atg13-independent mechanism. Mol Cell Biol *29*, 157-171.

Chang, Y.Y., and Neufeld, T.P. (2009). An Atg1/Atg13 complex with multiple roles in TOR-mediated autophagy regulation. Mol Biol Cell *20*, 2004-2014.

Cheong, H., Nair, U., Geng, J., and Klionsky, D.J. (2008). The Atg1 kinase complex is involved in the regulation of protein recruitment to initiate sequestering vesicle formation for nonspecific autophagy in Saccharomyces cerevisiae. Mol Biol Cell *19*, 668-681.

De Duve, C., and Wattiaux, R. (1966). Functions of lysosomes. Annu Rev Physiol *28*, 435-492.

Finley, D. (2009). Recognition and processing of ubiquitin-protein conjugates by the proteasome. Annu Rev Biochem *78*, 477-513.

Funakoshi, T., Matsuura, A., Noda, T., and Ohsumi, Y. (1997). Analyses of APG13 gene involved in autophagy in yeast, Saccharomyces cerevisiae. Gene *192*, 207-213.

Ganley, I.G., Lam du, H., Wang, J., Ding, X., Chen, S., and Jiang, X. (2009). ULK1.ATG13.FIP200 complex mediates mTOR signaling and is essential for autophagy. J Biol Chem *284*, 12297-12305.

Gronostajski, R.M., and Pardee, A.B. (1984). Protein degradation in 3T3 cells and tumorigenic transformed 3T3 cells. J Cell Physiol *119*, 127-132.

Harding, T.M., Morano, K.A., Scott, S.V., and Klionsky, D.J. (1995). Isolation and characterization of yeast mutants in the cytoplasm to vacuole protein targeting pathway. J Cell Biol *131*, 591-602.

He, C., and Klionsky, D.J. (2009). Regulation mechanisms and signaling pathways of autophagy. Annu Rev Genet *43*, 67-93.

Hosokawa, N., Hara, T., Kaizuka, T., Kishi, C., Takamura, A., Miura, Y., Iemura, S., Natsume, T., Takehana, K., Yamada, N.*, et al.* (2009a). Nutrient-dependent mTORC1 association with the ULK1-Atg13-FIP200 complex required for autophagy. Mol Biol Cell *20*, 1981-1991.

Hosokawa, N., Sasaki, T., Iemura, S., Natsume, T., Hara, T., and Mizushima, N. (2009b). Atg101, a novel mammalian autophagy protein interacting with Atg13. Autophagy *5*, 973-979.

Inoki, K., Li, Y., Xu, T., and Guan, K.L. (2003a). Rheb GTPase is a direct target of TSC2 GAP activity and regulates mTOR signaling. Genes Dev *17*, 1829-1834.

Inoki, K., Zhu, T., and Guan, K.L. (2003b). TSC2 mediates cellular energy response to control cell growth and survival. Cell *115*, 577-590.

Jung, C.H., Jun, C.B., Ro, S.H., Kim, Y.M., Otto, N.M., Cao, J., Kundu, M., and Kim, D.H. (2009). ULK-Atg13-FIP200 complexes mediate mTOR signaling to the autophagy machinery. Mol Biol Cell *20*, 1992-2003.

Kabeya, Y., Kamada, Y., Baba, M., Takikawa, H., Sasaki, M., and Ohsumi, Y. (2005). Atg17 functions in cooperation with Atg1 and Atg13 in yeast autophagy. Mol Biol Cell *16*, 2544-2553.

Kabeya, Y., Kawamata, T., Suzuki, K., and Ohsumi, Y. (2007). Cis1/Atg31 is required for autophagosome formation in Saccharomyces cerevisiae. Biochem Biophys Res Commun *356*, 405-410.

Kamada, Y. (2010). Prime-numbered Atg proteins act at the primary step in autophagy: unphosphorylatable Atg13 can induce autophagy without TOR inactivation. Autophagy *6*, 415-416.

Kamada, Y., Funakoshi, T., Shintani, T., Nagano, K., Ohsumi, M., and Ohsumi, Y. (2000). Tor-mediated induction of autophagy via an Apg1 protein kinase complex. J Cell Biol *150*, 1507-1513.

Kawamata, T., Kamada, Y., Kabeya, Y., Sekito, T., and Ohsumi, Y. (2008). Organization of the pre-autophagosomal structure responsible for autophagosome formation. Mol Biol Cell *19*, 2039-2050.

Kawamata, T., Kamada, Y., Suzuki, K., Kuboshima, N., Akimatsu, H., Ota, S., Ohsumi, M., and Ohsumi, Y. (2005). Characterization of a novel autophagy-specific gene, ATG29. Biochem Biophys Res Commun *338*, 1884-1889.

Kim, E., Goraksha-Hicks, P., Li, L., Neufeld, T.P., and Guan, K.L. (2008). Regulation of TORC1 by Rag GTPases in nutrient response. Nat Cell Biol *10*, 935-945.

Klionsky, D.J. (2007). Autophagy: from phenomenology to molecular understanding in less than a decade. Nat Rev Mol Cell Biol *8*, 931-937.

Kroemer, G., Marino, G., and Levine, B. (2010). Autophagy and the integrated stress response. Mol Cell *40*, 280-293.

Kuroyanagi, H., Yan, J., Seki, N., Yamanouchi, Y., Suzuki, Y., Takano, T., Muramatsu, M., and Shirasawa, T. (1998). Human ULK1, a novel serine/threonine kinase related to UNC-51 kinase of Caenorhabditis elegans: cDNA cloning, expression, and chromosomal assignment. Genomics *51*, 76-85.

Lee, J.W., Park, S., Takahashi, Y., and Wang, H.G. (2010). The association of AMPK with ULK1 regulates autophagy. PLoS One *5*, e15394.

Liang, J., Shao, S.H., Xu, Z.X., Hennessy, B., Ding, Z., Larrea, M., Kondo, S., Dumont, D.J., Gutterman, J.U., Walker, C.L*., et al.* (2007). The energy sensing LKB1-AMPK pathway regulates p27(kip1) phosphorylation mediating the decision to enter autophagy or apoptosis. Nat Cell Biol *9*, 218-224.

Liang, X.H., Jackson, S., Seaman, M., Brown, K., Kempkes, B., Hibshoosh, H., and Levine, B. (1999). Induction of autophagy and inhibition of tumorigenesis by beclin 1. Nature *402*, 672-676.

Liang, X.H., Kleeman, L.K., Jiang, H.H., Gordon, G., Goldman, J.E., Berry, G., Herman, B., and Levine, B. (1998). Protection against fatal Sindbis virus encephalitis by beclin, a novel Bcl-2-interacting protein. J Virol *72*, 8586-8596.

Long, X., Lin, Y., Ortiz-Vega, S., Yonezawa, K., and Avruch, J. (2005). Rheb binds and regulates the mTOR kinase. Curr Biol *15*, 702-713.

Lum, J.J., Bauer, D.E., Kong, M., Harris, M.H., Li, C., Lindsten, T., and Thompson, C.B. (2005). Growth factor regulation of autophagy and cell survival in the absence of apoptosis. Cell *120*, 237-248.

Manning, B.D., Tee, A.R., Logsdon, M.N., Blenis, J., and Cantley, L.C. (2002). Identification of the tuberous sclerosis complex-2 tumor suppressor gene product tuberin as a target of the phosphoinositide 3-kinase/akt pathway. Mol Cell *10*, 151-162.

Matsuura, A., Tsukada, M., Wada, Y., and Ohsumi, Y. (1997). Apg1p, a novel protein kinase required for the autophagic process in Saccharomyces cerevisiae. Gene *192*, 245-250.

Mercer, C.A., Kaliappan, A., and Dennis, P.B. (2009). A novel, human Atg13 binding protein, Atg101, interacts with ULK1 and is essential for macroautophagy. Autophagy *5*, 649-662.

Mizushima, N. (2010). The role of the Atg1/ULK1 complex in autophagy regulation. Curr Opin Cell Biol *22*, 132-139.

Mortimore, G.E., Poso, A.R., and Lardeux, B.R. (1989). Mechanism and regulation of protein degradation in liver. Diabetes Metab Rev *5*, 49-70.

Nakatogawa, H., Suzuki, K., Kamada, Y., and Ohsumi, Y. (2009). Dynamics and diversity in autophagy mechanisms: lessons from yeast. Nat Rev Mol Cell Biol *10*, 458-467.

Nicklin, P., Bergman, P., Zhang, B., Triantafellow, E., Wang, H., Nyfeler, B., Yang, H., Hild, M., Kung, C., Wilson, C.*, et al.* (2009). Bidirectional transport of amino acids regulates mTOR and autophagy. Cell *136*, 521-534.

Nobukuni, T., Joaquin, M., Roccio, M., Dann, S.G., Kim, S.Y., Gulati, P., Byfield, M.P., Backer, J.M., Natt, F., Bos, J.L.*, et al.* (2005). Amino acids mediate mTOR/raptor signaling through activation of class 3 phosphatidylinositol 3OH-kinase. Proc Natl Acad Sci U S A *102*, 14238-14243.

Noda, T., and Ohsumi, Y. (1998). Tor, a phosphatidylinositol kinase homologue, controls autophagy in yeast. J Biol Chem *273*, 3963-3966.

Okazaki, N., Yan, J., Yuasa, S., Ueno, T., Kominami, E., Masuho, Y., Koga, H., and Muramatsu, M. (2000). Interaction of the Unc-51-like kinase and microtubule-associated protein light chain 3 related proteins in the brain: possible role of vesicular transport in axonal elongation. Brain Res Mol Brain Res *85*, 1-12.

Sancak, Y., Bar-Peled, L., Zoncu, R., Markhard, A.L., Nada, S., and Sabatini, D.M. (2010). Ragulator-Rag complex targets mTORC1 to the lysosomal surface and is necessary for its activation by amino acids. Cell *141*, 290-303.

Sancak, Y., Peterson, T.R., Shaul, Y.D., Lindquist, R.A., Thoreen, C.C., Bar-Peled, L., and Sabatini, D.M. (2008). The Rag GTPases bind raptor and mediate amino acid signaling to mTORC1. Science *320*, 1496-1501.

Schwartz, A.L., and Ciechanover, A. (1999). The ubiquitin-proteasome pathway and pathogenesis of human diseases. Annu Rev Med *50*, 57-74.

Schworer, C.M., Shiffer, K.A., and Mortimore, G.E. (1981). Quantitative relationship between autophagy and proteolysis during graded amino acid deprivation in perfused rat liver. J Biol Chem *256*, 7652-7658.

Sekito, T., Kawamata, T., Ichikawa, R., Suzuki, K., and Ohsumi, Y. (2009). Atg17 recruits Atg9 to organize the pre-autophagosomal structure. Genes Cells *14*, 525-538.

Stokoe, D., Stephens, L.R., Copeland, T., Gaffney, P.R., Reese, C.B., Painter, G.F., Holmes, A.B., McCormick, F., and Hawkins, P.T. (1997). Dual role of phosphatidylinositol-3,4,5-trisphosphate in the activation of protein kinase B. Science *277*, 567-570.

Sumpter, R., Jr., and Levine, B. (2010). Autophagy and innate immunity: triggering, targeting and tuning. Semin Cell Dev Biol *21*, 699-711.

Suzuki, K., Kubota, Y., Sekito, T., and Ohsumi, Y. (2007). Hierarchy of Atg proteins in pre-autophagosomal structure organization. Genes Cells *12*, 209-218.

Takeshige, K., Baba, M., Tsuboi, S., Noda, T., and Ohsumi, Y. (1992). Autophagy in yeast demonstrated with proteinase-deficient mutants and conditions for its induction. J Cell Biol *119*, 301-311.

Thumm, M., Egner, R., Koch, B., Schlumpberger, M., Straub, M., Veenhuis, M., and Wolf, D.H. (1994). Isolation of autophagocytosis mutants of Saccharomyces cerevisiae. FEBS Lett *349*, 275-280.

Tsukada, M., and Ohsumi, Y. (1993). Isolation and characterization of autophagy-defective mutants of Saccharomyces cerevisiae. FEBS Lett *333*, 169-174.

Wang, Z., Wilson, W.A., Fujino, M.A., and Roach, P.J. (2001). Antagonistic controls of autophagy and glycogen accumulation by Snf1p, the yeast homolog of AMP-activated protein kinase, and the cyclin-dependent kinase Pho85p. Mol Cell Biol *21*, 5742-5752.

Wong, E., and Cuervo, A.M. (2010). Autophagy gone awry in neurodegenerative diseases. Nat Neurosci *13*, 805-811.

Wullschleger, S., Loewith, R., and Hall, M.N. (2006). TOR signaling in growth and metabolism. Cell *124*, 471-484.

Yorimitsu, T., He, C., Wang, K., and Klionsky, D.J. (2009). Tap42-associated protein phosphatase type 2A negatively regulates induction of autophagy. Autophagy *5*, 616-624.

Yorimitsu, T., and Klionsky, D.J. (2005). Autophagy: molecular machinery for self-eating. Cell Death Differ *12 Suppl 2*, 1542-1552.

Zhang, Y., Gao, X., Saucedo, L.J., Ru, B., Edgar, B.A., and Pan, D. (2003). Rheb is a direct target of the tuberous sclerosis tumour suppressor proteins. Nat Cell Biol *5*, 578-581.

Zhong, Q., Gao, W., Du, F., and Wang, X. (2005). Mule/ARF-BP1, a BH3-only E3 ubiquitin ligase, catalyzes the polyubiquitination of Mcl-1 and regulates apoptosis. Cell *121*, 1085-1095.